Electronic Supplementary Material (ESI) for Polymer Chemistry.

Supporting Information for

Tuning Properties of α,ω-Bis(trialkoxysilyl) Telechelic Copolyolefins from Ruthenium-Catalyzed Chain-Transfer Ring-Opening Metathesis Polymerization (ROMP)

Table S1. Apparent physical state and thermal analysis of different homopolyolefins synthesized by ROMP/CM using CTA **1** and catalyst **G2** in CH_2Cl_2 at 40 °C for 24 h; $[Monomer]_0/[CTA]_0/[\mathbf{G2}]_0 = 2000:100:1$.

Scheme S1. Different microstructures of PDCPD obtained from ROMP of DCPD.

Table S2. Copolymerization of NB-OLF and mOLF catalyzed by **G2** using CTA **1** in CH_2Cl_2 during 24 h*.

Fig. S1. SEC traces of copolyolefin samples prepared from the ROMP of NB/COE, NB^{COOMe}/COE, DCPD/CDT and DCPD/COD using **G2** catalyst and CTA **1** (Table 1, entries 1, 6, 12, 14).

Fig. S2. ^1H NMR spectrum (400 MHz, $CDCl_3$, 23 °C) of a crude copolymer prepared from ROMP/CM of NB^{COOMe} and COE using **G2** and CTA **1** (Table 1, entry 6).

Fig. S3. ^{13}C NMR spectrum (100 MHz, $CDCl_3$, 23 °C) of a crude copolymer prepared from ROMP/CM of NB^{COOMe} and COE using **G2** and CTA **1** (Table 1, entry 6).

Fig. S4. FTIR spectrum of a crude copolymer prepared from ROMP/CM of NB^{COOMe} and COE using **G2** and CTA **1** (Table 1, entry 6).

Fig. S5. ^1H NMR spectrum (500 MHz, $CDCl_3$, 23 °C) of a crude copolymer prepared from ROMP/CM of $oxaNB^{COOMe}$ and COE using **G2** and CTA **1** (Table 1, entry 8).

Fig. S6. $^{13}C\{^1H\}$ NMR spectrum (125 MHz, $CDCl_3$, 23 °C) of a crude copolymer prepared from ROMP/CM of $oxaNB^{COOMe}$ and COE using **G2** and CTA **1** (Table 1, entry 8).

Fig. S7. FTIR spectrum of a crude copolymer prepared from ROMP/CM of $oxaNB^{COOMe}$ and COE using **G2** and CTA **1** (Table 1, entry 8).

Fig. S8. ^1H NMR spectrum (500 MHz, $CDCl_3$, 23 °C) of a crude copolymer prepared from ROMP/CM of NB and CDT using **G2** and CTA **1** (Table 1, entry 3).

Fig. S9. $^{13}C\{^1H\}$ NMR spectrum (125 MHz, $CDCl_3$, 23 °C) of a crude copolymer prepared from ROMP/CM of NB and CDT using **G2** and CTA **1** (Table 1, entry 3).

Fig. S10. FTIR spectrum of a crude copolymer prepared from ROMP/CM of NB and CDT using **G2** and CTA **1** (Table 1, entry 3).

Fig.S11. ^{1}H NMR spectrum (400 MHz, $CDCl_3$, 23 °C) of **CNF** copolymer isolated from a crude copolymer prepared from ROMP/CM of NB and CDT using **G2** and CTA **1** (Table 1, entry 3).

Fig. S12. $^{13}C\{^{1}H\}$ NMR spectrum (100 MHz, $CDCl_3$, 23 °C) of **CNF** copolymer isolated from a crude copolymer prepared from ROMP/CM of NB and CDT using **G2** and CTA **1** (Table 1, entry 3).

Fig.S13. ^{1}H NMR spectrum (400 MHz, $CDCl_3$, 23 °C) of a crude copolymer prepared from ROMP/CM of ENB and CDT using **G2** and CTA **1** (Table 1, entry 4).

Fig. S14. $^{13}C\{^{1}H\}$ NMR spectrum (100 MHz, $CDCl_3$, 23 °C) of a crude copolymer prepared from ROMP/CM of ENB and CDT using **G2** and CTA **1** (Table 1, entry 4).

Fig.S15. FTIR spectrum of a crude copolymer prepared from ROMP/CM of ENB and CDT using **G2** and CTA **1** (Table 1, entry 4).

Fig. S16. ^{1}H NMR spectrum (400 MHz, $CDCl_3$, 23 °C) of **CNF** copolymer isolated from a crude copolymer prepared from ROMP/CM of ENB and CDT using **G2** and CTA **1** (Table 1, entry 4).

Fig. S17. $^{13}C\{^{1}H\}$ NMR spectrum (125 MHz, $CDCl_3$, 23 °C) of **CNF** copolymer isolated from a crude copolymer prepared from ROMP/CM of ENB and CDT using **G2** and CTA **1** (Table 1, entry 4).

Fig.S18. ^{1}H NMR spectrum (500 MHz, $CDCl_3$, 23 °C) of a crude copolymer prepared from ROMP/CM of DCPD and COE using **G2** and CTA **1** (Table 1, entry 10).

Fig.S19. $^{13}C\{^{1}H\}$ NMR spectrum (125 MHz, $CDCl_3$, 23 °C) of a crude copolymer prepared from ROMP/CM of DCPD and COE using **G2** and CTA **1** (Table 1, entry 10).

Fig. S20. FTIR spectrum of a crude copolymer prepared from ROMP/CM of DCPD and COE using **G2** and CTA **1** (Table 1, entry 10).

Fig. S21. ^{1}H NMR spectrum (500 MHz, $CDCl_3$, 23 °C) of **CNF** copolymer isolated from a crude copolymer prepared from ROMP/CM of DCPD and COE using **G2** and CTA **1** (Table 1, entry 10).

Fig.S22. $^{13}C\{^{1}H\}$ NMR spectrum (125 MHz, $CDCl_3$, 23 °C) of **CNF** copolymer isolated from a crude copolymer prepared from ROMP/CM of DCPD and COE using **G2** and CTA **1** (Table 1, entry 10).

Fig. S23. ^{1}H NMR spectrum (500 MHz, $CDCl_3$, 23 °C) of a crude copolymer prepared from ROMP/CM of DCPD and CDT using **G2** and CTA **1** (Table 1, entry 12).

Fig. S24. $^{13}C\{^{1}H\}$ NMR spectrum (125 MHz, $CDCl_3$, 23 °C) of a crude copolymer prepared from ROMP/CM of DCPD and CDT using **G2** and CTA **1** (Table 1, entry 12).

Fig. S25. FTIR spectrum of a crude copolymer prepared from ROMP/CM of DCPD and CDT using **G2** and CTA **1** (Table 1, entry 12).

Fig. S26. ^{1}H NMR spectrum (500 MHz, $CDCl_3$, 23 °C) of a crude copolymer prepared from ROMP/CM of DCPD and COD using **G2** and CTA **1** (Table 1, entry 14).

Fig. S27. $^{13}C\{^{1}H\}$ NMR spectrum (125 MHz, $CDCl_3$, 23 °C) of a crude copolymer prepared from ROMP/CM of DCPD and COD using **G2** and CTA **1** (Table 1, entry 14).

Fig. S28. FTIR spectrum of a crude copolymer prepared from ROMP/CM of DCPD and COD using **G2** and CTA **1** (Table 1, entry 14).

Fig. S29. ^{1}H NMR spectrum (500 MHz, $CDCl_3$, 23 °C) of **CNF** copolymer isolated from a crude copolymer prepared from ROMP/CM of DCPD and COD using **G2** and CTA **1** (Table 1, entry 14).

Fig. S30. $^{13}C\{^{1}H\}$ NMR spectrum (125 MHz, $CDCl_3$, 23 °C) of **CNF** copolymer isolated from a crude copolymer prepared from ROMP/CM of DCPD and COD using **G2** and CTA **1** (Table 1, entry 14).

Fig. S31. ^{1}H NMR spectrum (400 MHz, $CDCl_3$, 23 °C) of **CNF** copolymer isolated from a crude copolymer prepared from ROMP/CM of NB and COE using **G2** and CTA **1-OEt** (Table 1, entry 1).

Fig. S32. ^{13}C NMR spectrum (100 MHz, $CDCl_3$, 23 °C) of **CNF** copolymer isolated from a crude copolymer prepared from ROMP/CM of NB and COE using **G2** and CTA **1-OEt** (Table 1, entry 1).

Fig. S33. ^{1}H-$^{13}C\{^{1}H\}$ HMBC (DEPT) NMR spectrum (400 MHz, $CDCl_3$, 23 °C) of a crude copolymer prepared from ROMP/CM of NB and COE using **G2** and CTA **1** (Table 1, entry 1).

Fig. S34. ^{1}H-^{13}C HMBC (DEPT) NMR spectrum (400 MHz, $CDCl_3$, 23 °C) of a crude copolymer prepared from ROMP/CM of NB and CDT using **G2** and CTA **1** (Table 1, entry 3; spectrum with assignments of all signals in Fig. S35).

Fig. S35. ^{1}H-^{13}C HMBC (DEPT) NMR spectrum (400 MHz, $CDCl_3$, 23 °C) of a crude copolymer prepared from ROMP/CM of NB and CDT using **G2** and CTA **1** (Table 1, entry 3).

Fig. S36. ^{1}H-^{13}C HMBC (DEPT) NMR spectrum (400 MHz, $CDCl_3$, 23 °C) of a crude copolymer prepared from ROMP/CM of ENB and CDT using **G2** and CTA **1** (Table 1, entry 4; spectrum with assignments of all signals in Fig. S37).

Fig. S37. ^{1}H-^{13}C HMBC (DEPT) NMR spectrum (400 MHz, $CDCl_3$, 23 °C) of a crude copolymer prepared from ROMP/CM of ENB and CDT using **G2** and CTA **1** (Table 1, entry 4).

Fig. S38. ^{1}H-^{13}C HMBC (DEPT) NMR spectrum (400 MHz, $CDCl_3$, 23 °C) of a crude copolymer prepared from ROMP/CM of oxaNB^{COOMe} and COE using **G2** and CTA **1** (Table 1, entry 8; spectrum with assignments of all signals in Fig.S39).

Fig. S39. ^{1}H-^{13}C HMBC (DEPT) NMR spectrum (400 MHz, $CDCl_3$, 23 °C) of a crude copolymer prepared from ROMP/CM of oxaNB^{COOMe} and COE using **G2** and CTA **1** (Table 1, entry 8).

Fig. S40. ^{1}H-^{13}C (DEPT) HMBC NMR spectrum (400 MHz, $CDCl_3$, 23 °C) of a crude copolymer prepared from ROMP/CM of oxaNB^{COOMe}/COE using **G2** and CTA **1** (Table 1, entry 10).

Fig. S41. FTIR spectrum of a crude copolymer prepared from ROMP/CM of NB and COE using **G2** and CTA **1** (Table 1, entry 1).

Fig. S42. DSC traces of copolyolefin samples prepared from the ROMP/CM of NB/CDT, oxaNB^{COOMe}/COE, DCPD/COE and DCPD/CDT using **G2** catalyst and CTA **1** (Table 2, entries 4, 6, 19, 24, 26, 31).

Fig. S43. Flow curves of copolyolefin samples prepared from the ROMP/CM of NB/COE, using **G2** catalyst and CTA **1** (Table 3, entries 1 and 2).

Fig. S44. Flow curves of copolyolefin samples prepared from the ROMP/CM of NB^{COOMe}/COE using **G2** catalyst and CTA **1** (Table 3, entries 3–6).

Fig. S45. Flow curves of copolyolefin samples prepared from the ROMP/CM of oxaNB^{COOMe}/COE using **G2** catalyst and CTA **1** (Table 3, entries 7–9).

Fig. S46. Flow curves of copolyolefin samples prepared from the ROMP/CM of DCPD/COE and DCPD/COD using **G2** catalyst and CTA **1** (Table 3, entries 10–12).

Fig. S47. ^{1}H NMR spectrum (500 MHz, $CDCl_3$, 23 °C) of oxaNB^{COOMe}.

Fig. S48. $^{13}C\{^{1}H\}$ NMR spectrum (125 MHz, $CDCl_3$, 23 °C) of oxaNB^{COOMe}.

Table S1. Apparent physical state and thermal analysis of different homopolyolefins synthesized by ROMP/CM using CTA **1** and catalyst **G2** in CH_2Cl_2 at 40 °C for 24 h; $[Monomer]_0/[CTA]_0/[\mathbf{G2}]_0 = 2000:100:1$.

Entry	Monomer	CTA **1-R**	$M_{n,theo}$ [b] (g.mol^{-1})	$M_{n,NMR}$ [c] (g.mol^{-1})	Apparent physical state at 23 °C	T_g [d] (°C)	T_m [d] (°C)	T_c [d] (°C)
1	COE	**OMe**	2200	2900	Solid	–78	52	45
2	CDT	**OEt**	3200	3200	Solid	*n.o.*	32	22
3	COD	**OEt**	2200	2500	Solid	*n.o.*	32	21
4	NB	**OEt**	3800	4500	Solid	32	-	-
5	ENB	**OEt**	-	-	Solid	110	-	-
6 [a]	DCPD	**OMe**	-	-	Solid	155	-	-
7	NB^{COOMe}	**OMe**	3000	2300	Liquid	–12	-	-
8	$oxaNB^{COOMe}$	**OMe**	3100	3500	Liquid	–2	-	-

[a] ROMP of DCPD was performed at 23 °C. [b] Theoretical molar mass value calculated from $M_{n,theo} = M_{monomer} \times (Conv.monomer \times [monomer]_0) / (Conv.\mathbf{CTA} \times [\mathbf{CTA}]_0)$, on the basis of the sole formation of functionalized copolymers, i.e. without taking into account any **CNF**. [c] Experimental molar mass value determined by ^{1}H NMR analysis (refer to the Experimental Section). In entries 1–4, 7 and 8, quantitative monomer and CTA conversion was observed by ^{1}H NMR analysis. In entries 5 and 6, quantitative monomer conversion was observed by ^{1}H NMR analysis; yet, the CTA was not consumed at all, thus precluding the determination of NMR molar mass values. [d] DSC experiments recorded according to the following cycles: −100 to +100 °C at 10 °C min^{-1}; +100 to −100 °C at 10 °C min^{-1}. *n.o.* = not observed.

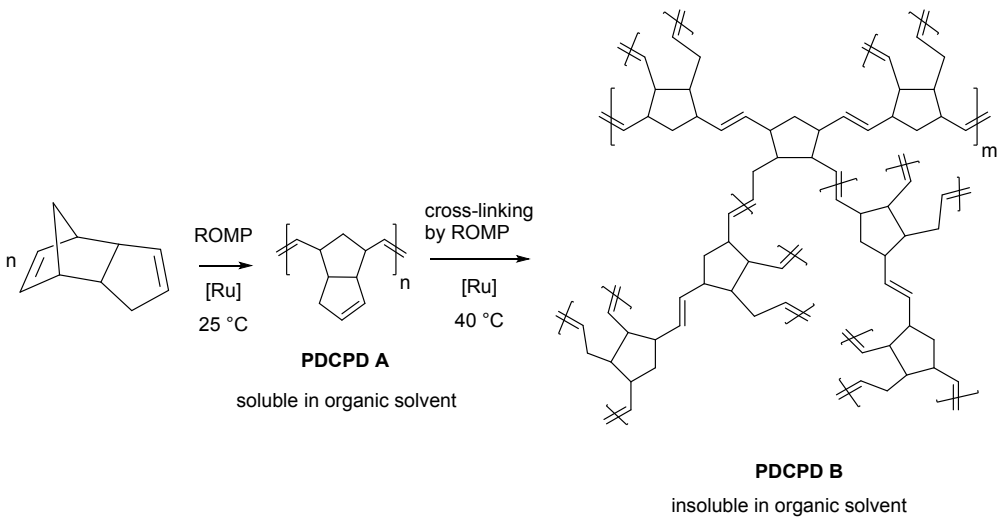

Scheme S1. Different microstructures of PDCPD obtained from the ROMP of DCPD. [Le Gac, P. Y.; Choqueuse, D.; Paris, M.; Recher, G.; Zimmer, C.; Melot, D. *Polym. Degrad. Stabil.,* **2013**, *98*, 809–817; Mohite, D. P.; Mahadik-Khanolkar, S.; Luo, H.; Lu, H.; Sotiriou-Leventis, C.; Leventis, N. *Soft Matter,* **2013**, *9*, 1516–1530; Davidson, T. A.; Wagener, K. B.; Priddy, D. B. *Macromolecules*, **1996**, *29*, 786–788; Yang, Y.-S. *Polymer*, **1997**, *38*, 1121–1130.]

Due to the different ring strain, the ROMP of DCPD usually first occurs via opening of the NB unit leading to **PDCPD A**, which is soluble in usual organic solvents. Then, cyclopentene rings can open, thus forming a cross-linked PDCPD network (**PDCPD B**). Copolymers containing **PDCPD B** are rigid (not liquid) at room temperature, and are thus not suitable for adhesive applications. Decreasing the reaction temperature to room temperature was found to enable the sole formation of **PDCPD A**. Therefore, all copolymerizations using DCPD as a comonomer were performed at 23 °C.

Table S2. Copolymerization of NB-OLF and mOLF catalyzed by **G2** using CTA **1** in CH_2Cl_2 during 24 h.*

Entry	Reaction Temp. (°C)	NB-OLF /mOLF	$[NB\text{-}OLF]_0$: $[mOLF]_0$	R-CTA **1**	$[CTA\ \mathbf{1}]_0$ (equiv vs **G2**)	NB-OLF Conv.[a] (mol%)	mOLF Conv.[a] (mol%)	DF Sel.[b] (wt%)	CNF Sel.[b] (wt%)	$M_{n,theo}$[c] (**DF**, g.mol^{-1})	$M_{n,NMR}$[d] (**DF**, g.mol^{-1})	$M_{n,SEC}$[e] (**DF**, g.mol^{-1})	$Đ_M$[e] (**DF**)	$M_{n,SEC}$[e] (**CNF**, g.mol^{-1})	$Đ_M$[e] (**CNF**)
1	40	NB/COE	1000:1000	**OEt**	50	100	100	97	3	4 100	4 100	10 700	1.7	13 200	1.5
2	40	NB/COE	25 000:25 000	**OEt**	1 250	100	100	83	17	4 100	4 500	21 700	1.7	22 800	1.6
3	40	NB/CDT	25 000:25 000	**OEt**	1 250	100	100	94	6	5 100	5 900	15 500	1.7	24 100	1.3
6	40	ENB/CDT	1000:1000	**OEt**	50	100	100	90	10	5 600	5 200	7 800	2.0	10 500	2.1
7	40	ENB/CDT	25 000:25 000	**OEt**	425	100	100	82	18	16 600	17 200	27 200	1.9	31 000	1.7
8	40	NB^{COOMe}/COE	1000:1000	**OMe**	50	100	100	98	2	5 200	5 500	13 600	1.5	14 400	1.5
9	40	NB^{COOMe}/COE	25 000:25 000	**OMe**	1 250	100	100	98	2	5 200	5 100	30 300	1.6	47 000	1.7
10	40	$oxaNB^{COOMe}$/COE	1000:1000	**OMe**	50	100	100	97	3	3 100	3 500	3 200	1.6	12 100	1.3
11	40	$oxaNB^{COOMe}$/COE	25 000:25 000	**OMe**	1 250	100	100	90	10	2 900	4 200	19 500	1.4	52 500	1.6
12	40	$oxaNB^{COOMe}$/COE	25 000:25 000	**OMe**	1 250	100	100	91	9	2 900	3 900	24 500	1.7	48 100	1.6
13	23	DCPD/COE	1000:1000	**OMe**	100	100	100	94	6	2 400	3 200	18 200	1.7	21 200	1.4
14	23	DCPD/COE	25 000:25 000	**OMe**	1 250	97	85	83	17	4 400	5 100	21 000	1.8	39 600	1.8
15	23	DCPD/CDT	1000:1000	**OEt**	100	100	100	97	3	2 900	4 600	11 200	2.0	25 000	1.5
16	23	DCPD/CDT	25 000:25 000	**OEt**	1 250	92	78	90	10	3 700	4 600	37 000	1.9	41 000	1.4
17[f]	23	DCPD/CDT	25 000:25 000	**OEt**	1 250	100	80	88	12	3 700	4 100	38 600	1.9	42 300	1.5
18	23	DCPD/COD	1000:1000	**OEt**	100	100	100	89	11	2 700	3 400	17 500	1.7	20 100	1.5

* Duplicated results of Table 1; NB, COE and CDT were distilled over CaH_2 prior to use; NB^{COOMe} and ENB were used as received; 1 equiv. of **G2** used in each reaction [a] Monomer and CTA conversion as determined by NMR analysis (refer to the Experimental Section). Full conversion of CTA was observed for all reactions [b] **DF** = difunctionalized copolymer; **CNF** = cyclic non-functionalized copolymer determined after weighting the CNF recovered following elution of the crude sample through a silica column (refer to the Experimental Section) (Scheme 1). [c] Theoretical molar mass value calculated from $M_{n,theo} = M_{monomer} \times (\text{Conv.monomer} \times [\text{monomer}]_0) / (\text{Conv.}\mathbf{CTA} \times [\mathbf{CTA}]_0)$, on the basis of the formation of only functionalized copolymers without taking into account any **CNF**. [d] Experimental molar mass value determined by ^{1}H NMR analysis (refer to the Experimental Section). [e] Number-average molar mass ($M_{n,SEC}$) and

dispersity ($Đ_M = M_w/M_n$) values determined by SEC *vs.* polystyrene standards (uncorrected M_n values) in THF at 30 °C. [f] ½ equiv. of catalyst was added at the beginning of the reaction, the other ½ equiv. was added after 24 h.

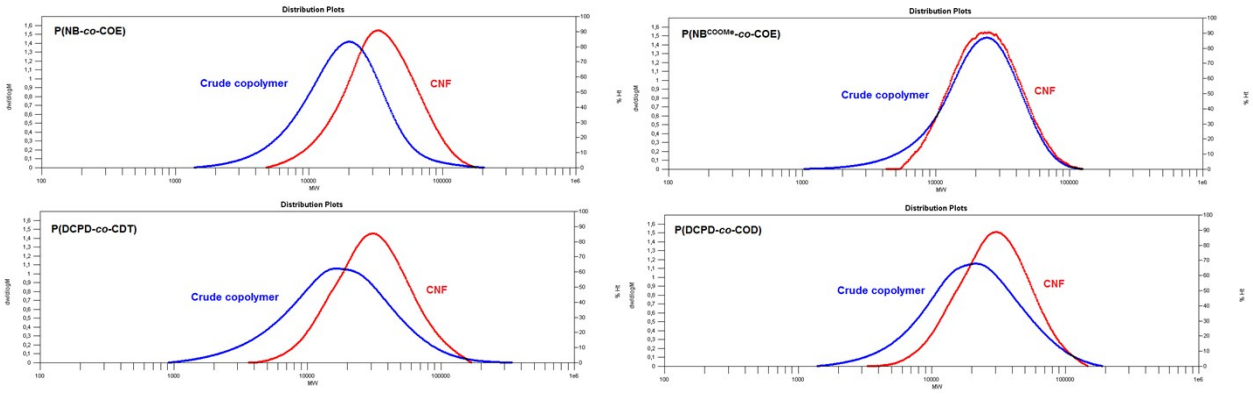

Fig. S1. SEC traces of copolyolefin samples prepared from the ROMP of NB/COE, NB^{COOMe}/COE, DCPD/CDT and DCPD/COD using **G2** catalyst and CTA **1** (Table 1, entries 1, 6, 12, 14).

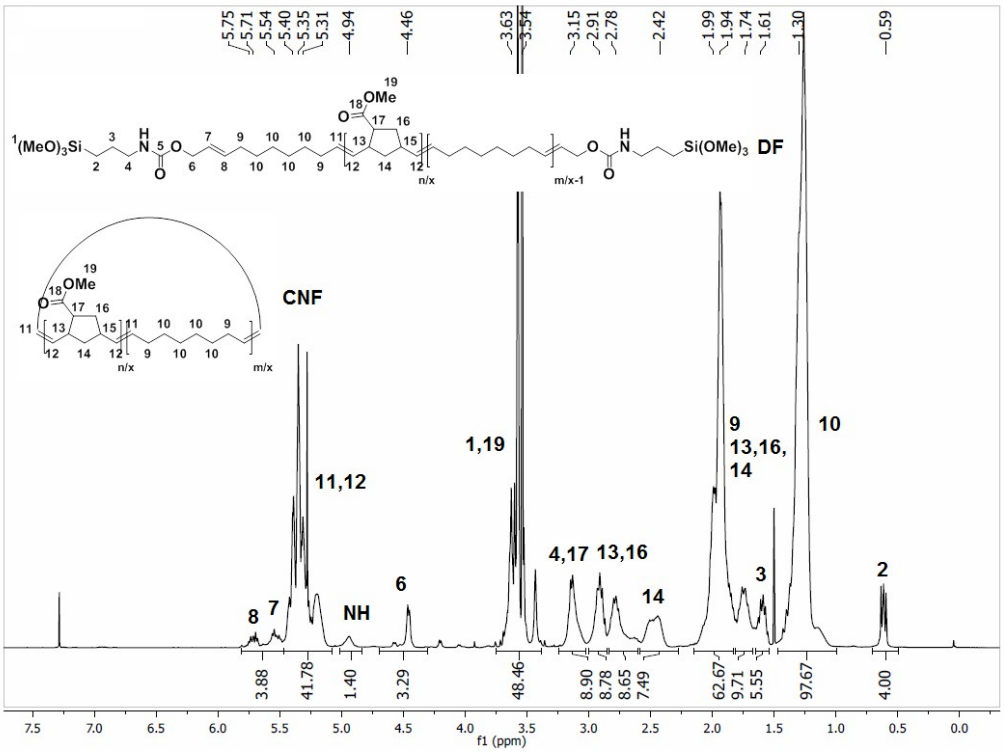

Fig. S2. ^{1}H NMR spectrum (400 MHz, $CDCl_3$, 23 °C) of a crude copolymer prepared from ROMP/CM of NB^{COOMe} and COE using **G2** and CTA **1** (Table 1, entry 6).

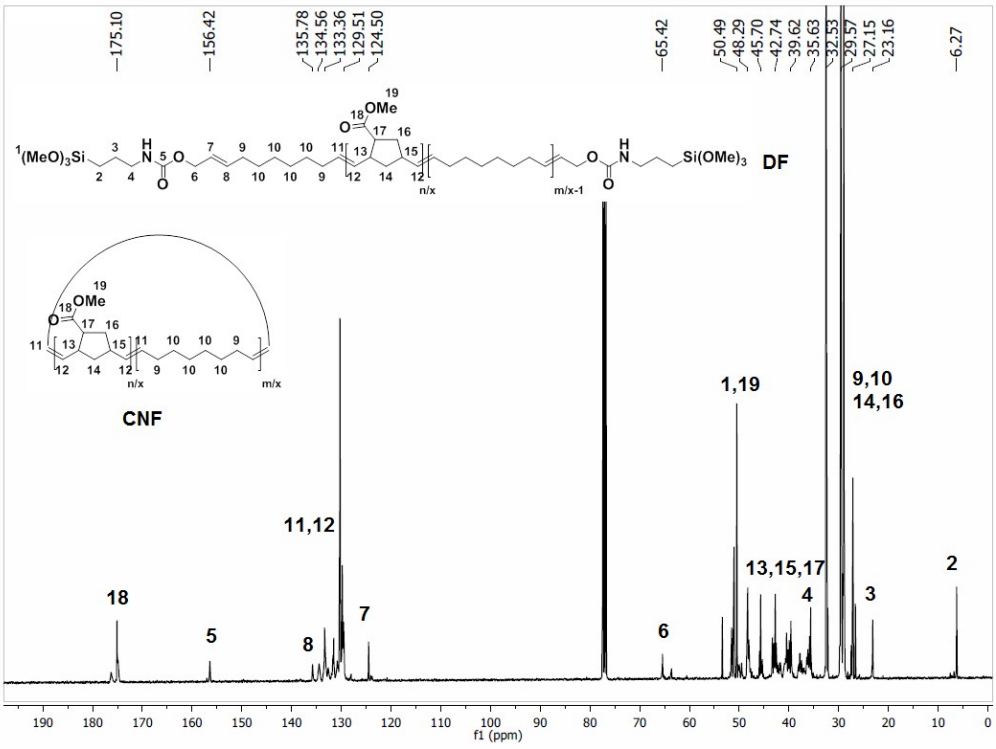

Fig. S3. ^{13}C NMR spectrum (100 MHz, $CDCl_3$, 23 °C) of a crude copolymer prepared from ROMP/CM of NB^{COOMe} and COE using **G2** and CTA **1** (Table 1, entry 6).

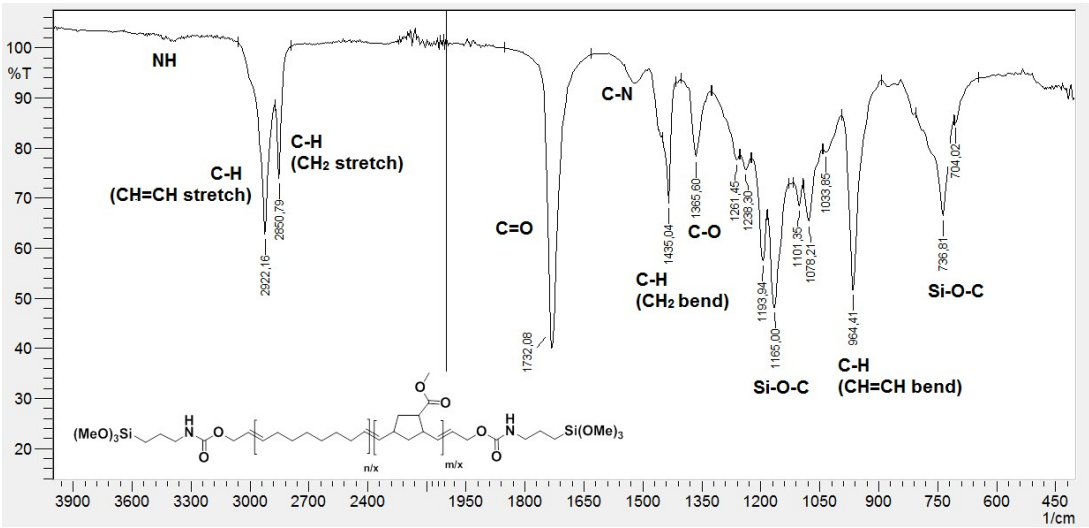

Fig. S4. FTIR spectrum of a crude copolymer prepared from ROMP/CM of NB^{COOMe} and COE using **G2** and CTA **1** (Table 1, entry 6).

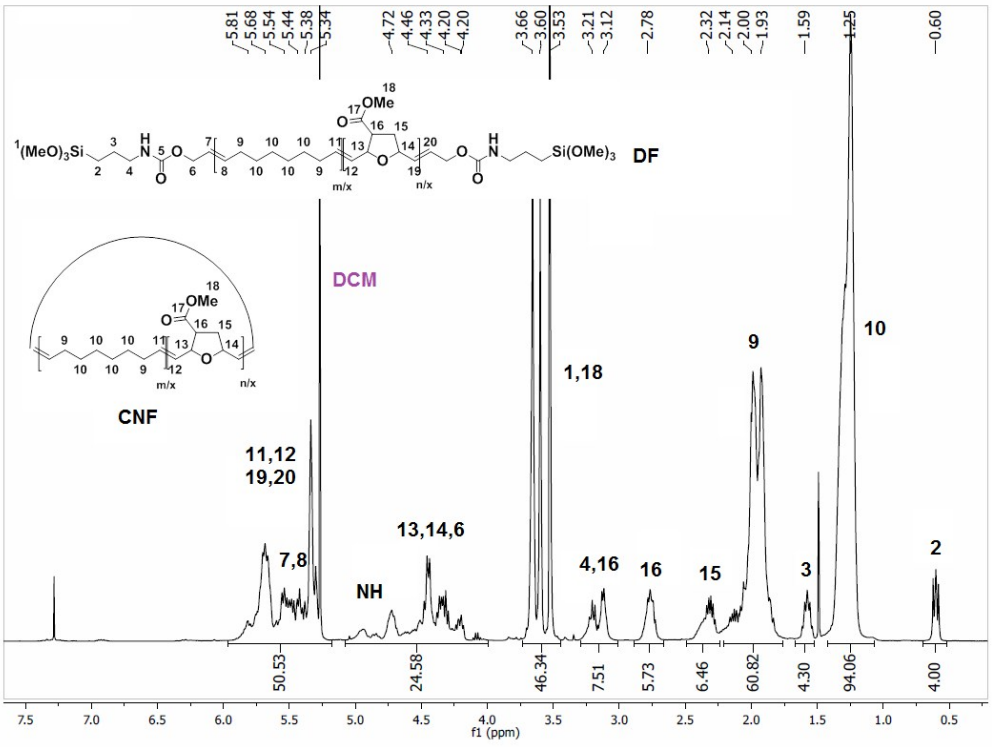

Fig. S5. ^{1}H NMR spectrum (500 MHz, $CDCl_3$, 23 °C) of a crude copolymer prepared from ROMP/CM of oxaNB^{COOMe} and COE using **G2** and CTA **1** (Table 1, entry 8).

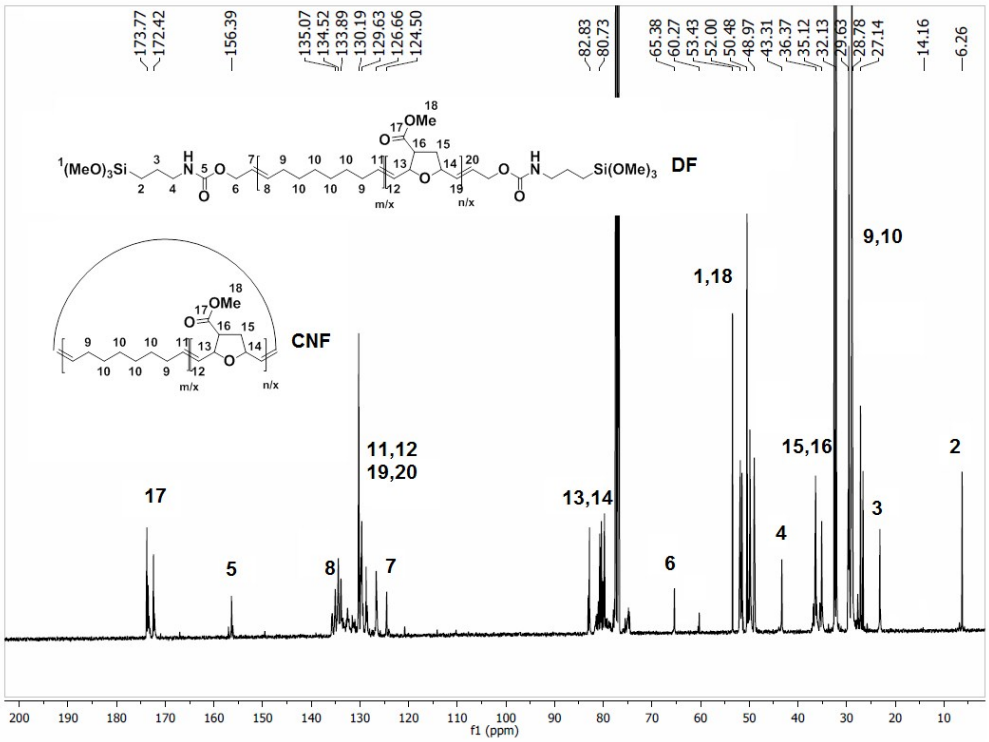

Fig. S6. ^{13}C{^{1}H} NMR spectrum (125 MHz, $CDCl_3$, 23 °C) of a crude copolymer prepared from ROMP/CM of oxaNB^{COOMe} and COE using **G2** and CTA **1** (Table 1, entry 8).

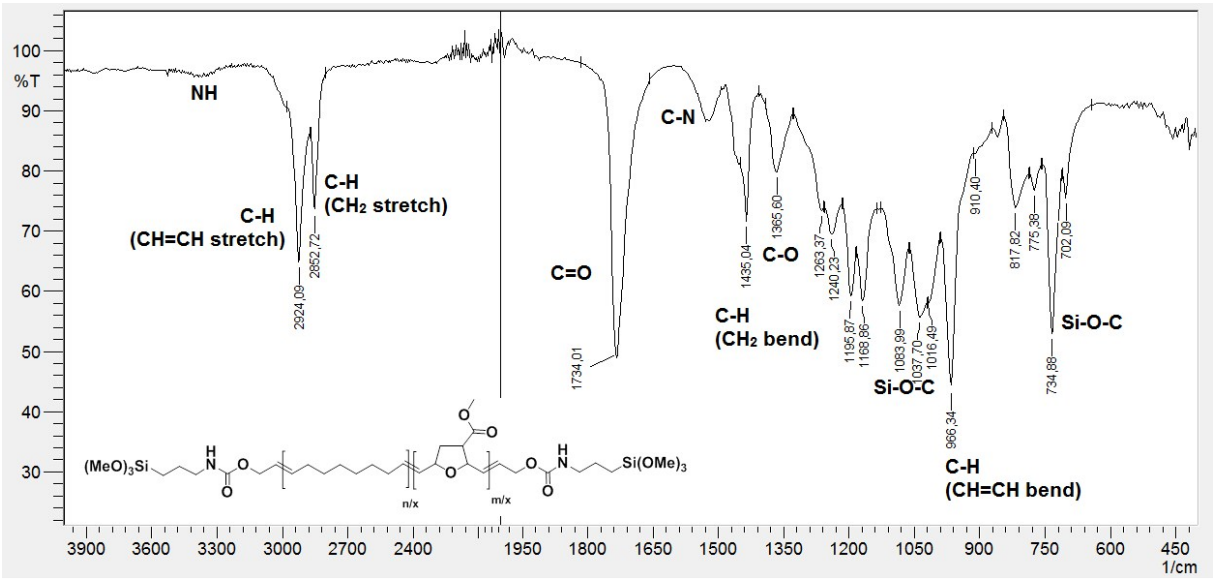

Fig. S7. FTIR spectrum of a crude copolymer prepared from ROMP/CM of oxaNB^{COOMe} and COE using **G2** and CTA **1** (Table 1, entry 8).

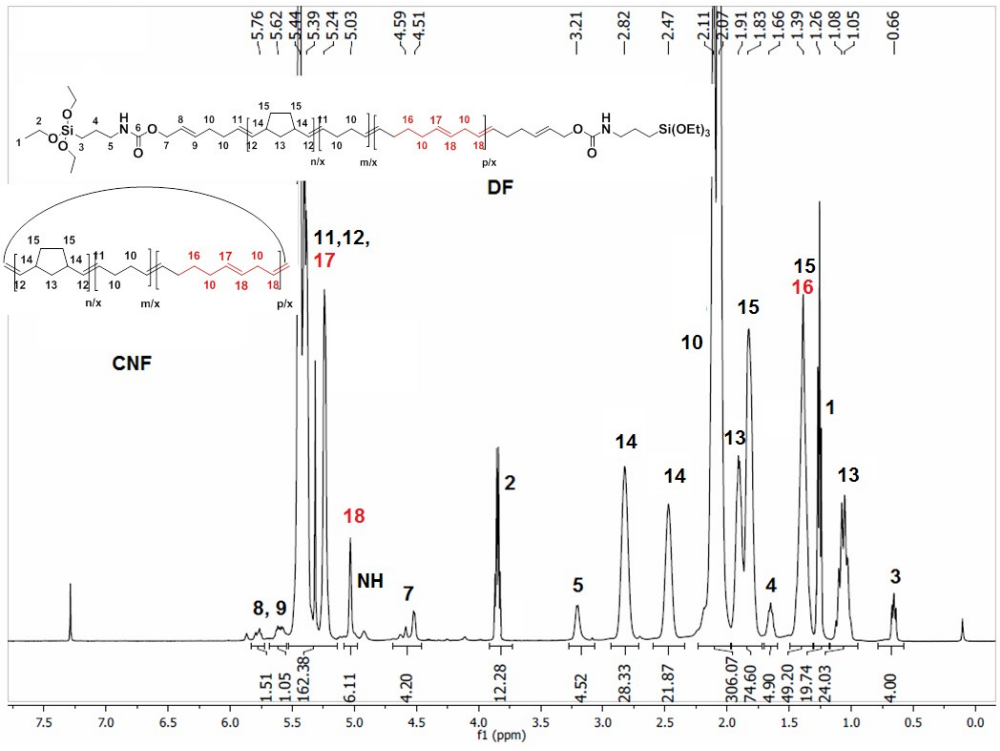

Fig. S8. ^{1}H NMR spectrum (500 MHz, $CDCl_3$, 23 °C) of a crude copolymer prepared from ROMP/CM of NB and CDT using **G2** and CTA **1** (Table 1, entry 3).

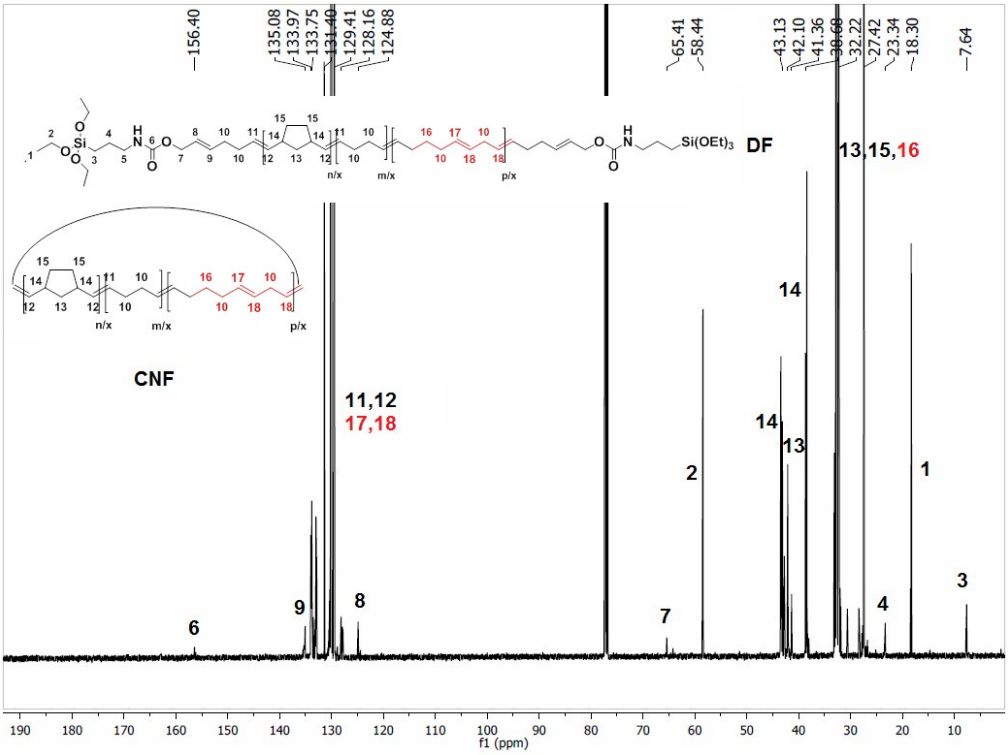

Fig. S9. $^{13}C\{^{1}H\}$ NMR spectrum (125 MHz, $CDCl_3$, 23 °C) of a crude copolymer prepared from ROMP/CM of NB and CDT using **G2** and CTA **1** (Table 1, entry 3).

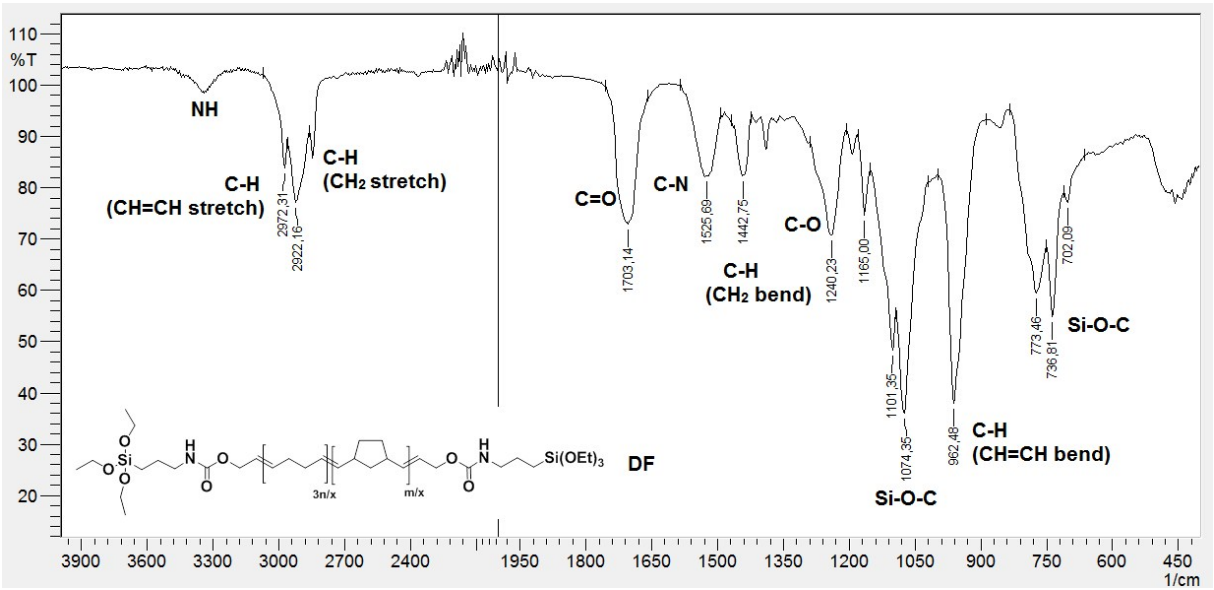

Fig. S10. FTIR spectrum of a crude copolymer prepared from ROMP/CM of NB and CDT using **G2** and CTA **1** (Table 1, entry 3).

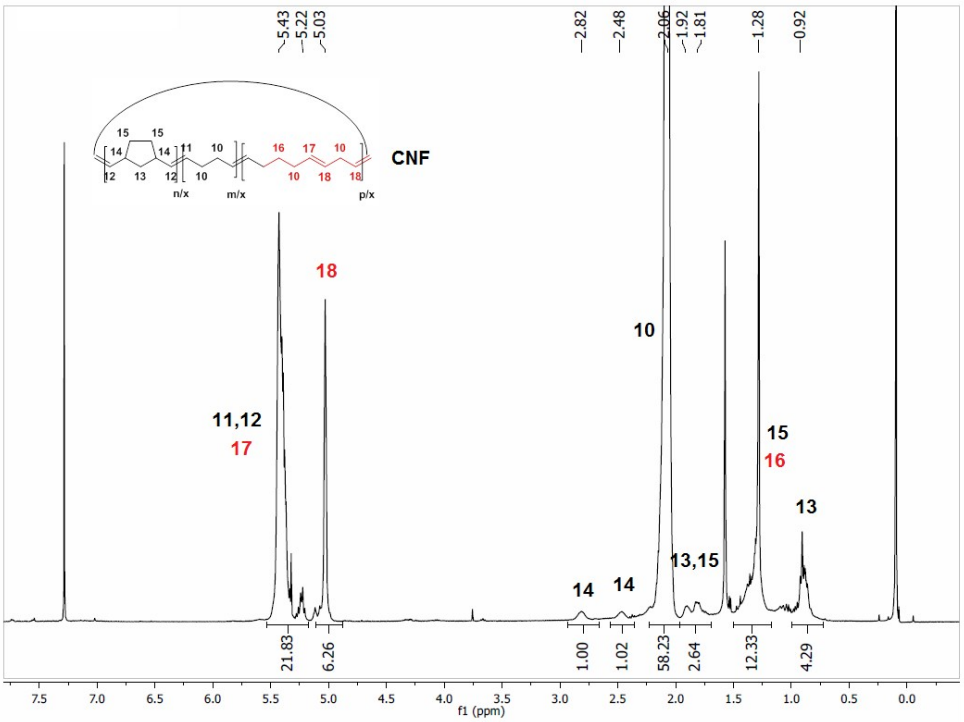

Fig.S11. ^{1}H NMR spectrum (400 MHz, $CDCl_3$, 23 °C) of **CNF** copolymer isolated from a crude copolymer prepared from ROMP/CM of NB and CDT using **G2** and CTA **1** (Table 1, entry 3).

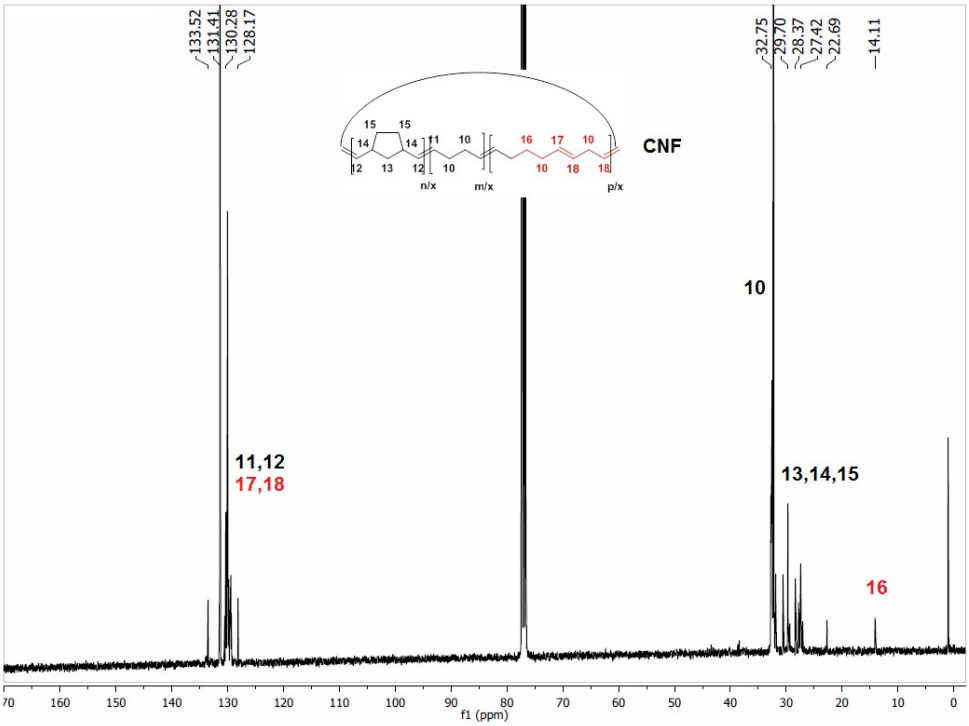

Fig. S12. $^{13}C\{^{1}H\}$ NMR spectrum (100 MHz, $CDCl_3$, 23 °C) of **CNF** copolymer isolated from a crude copolymer prepared from ROMP/CM of NB and CDT using **G2** and CTA **1** (Table 1, entry 3).

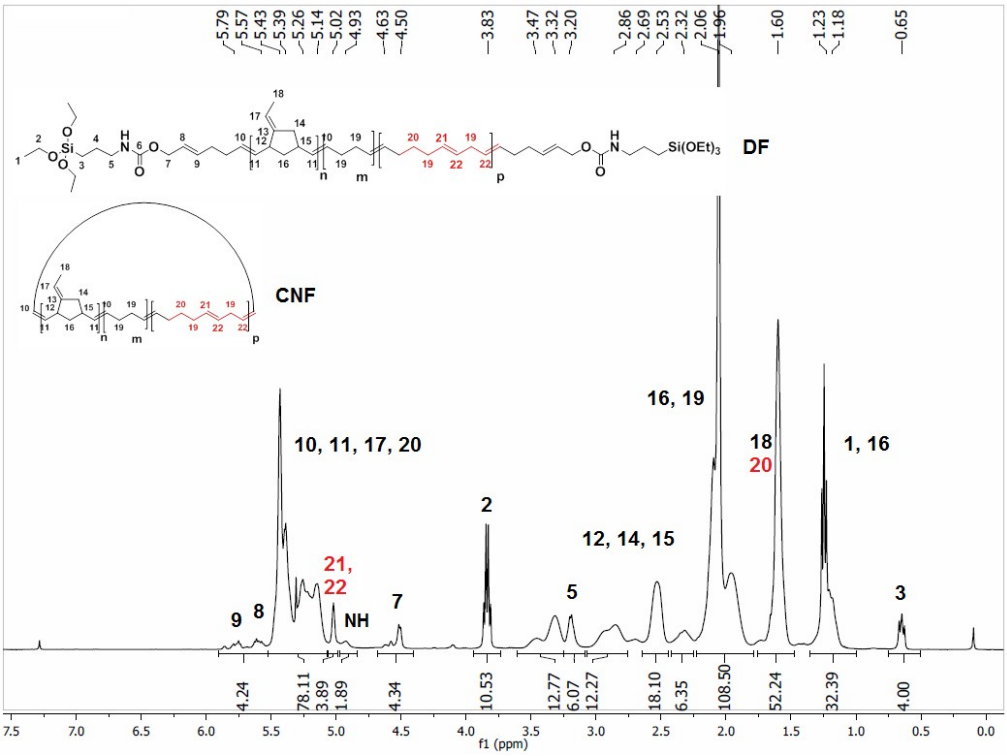

Fig.S13. ^{1}H NMR spectrum (400 MHz, $CDCl_3$, 23 °C) of a crude copolymer prepared from ROMP/CM of ENB and CDT using **G2** and CTA **1** (Table 1, entry 4).

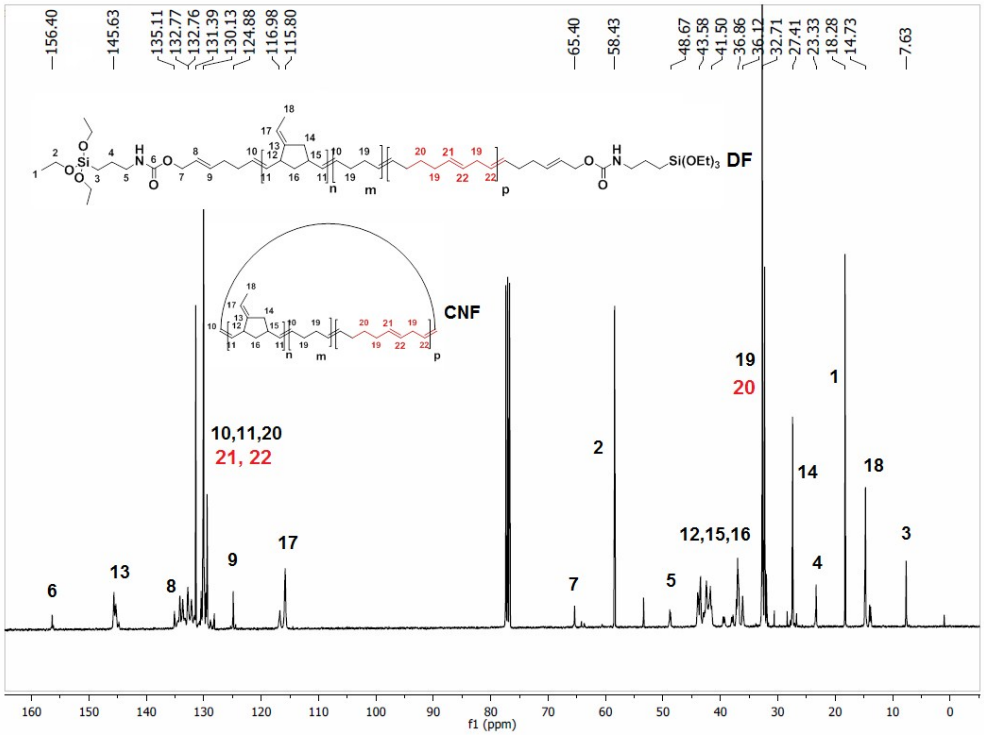

Fig. S14. $^{13}C\{^{1}H\}$ NMR spectrum (100 MHz, $CDCl_3$, 23 °C) of a crude copolymer prepared from ROMP/CM of ENB and CDT using **G2** and CTA **1** (Table 1, entry 4).

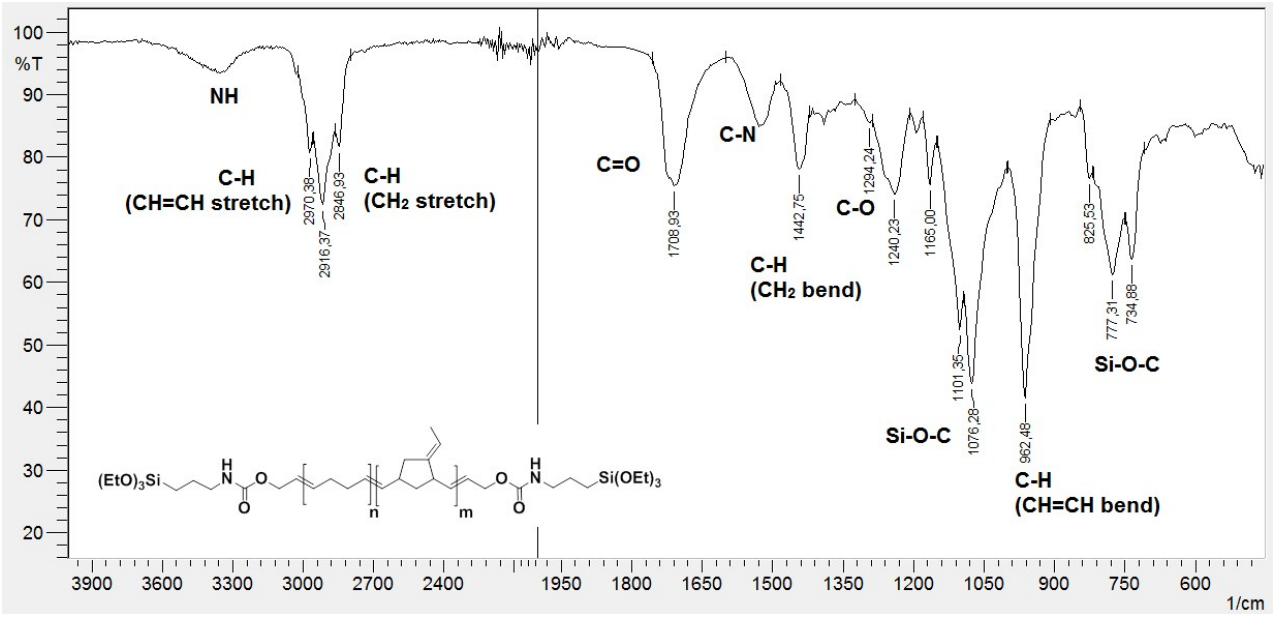

Fig.S15. FTIR spectrum of a crude copolymer prepared from ROMP/CM of ENB and CDT using **G2** and CTA **1** (Table 1, entry 4).

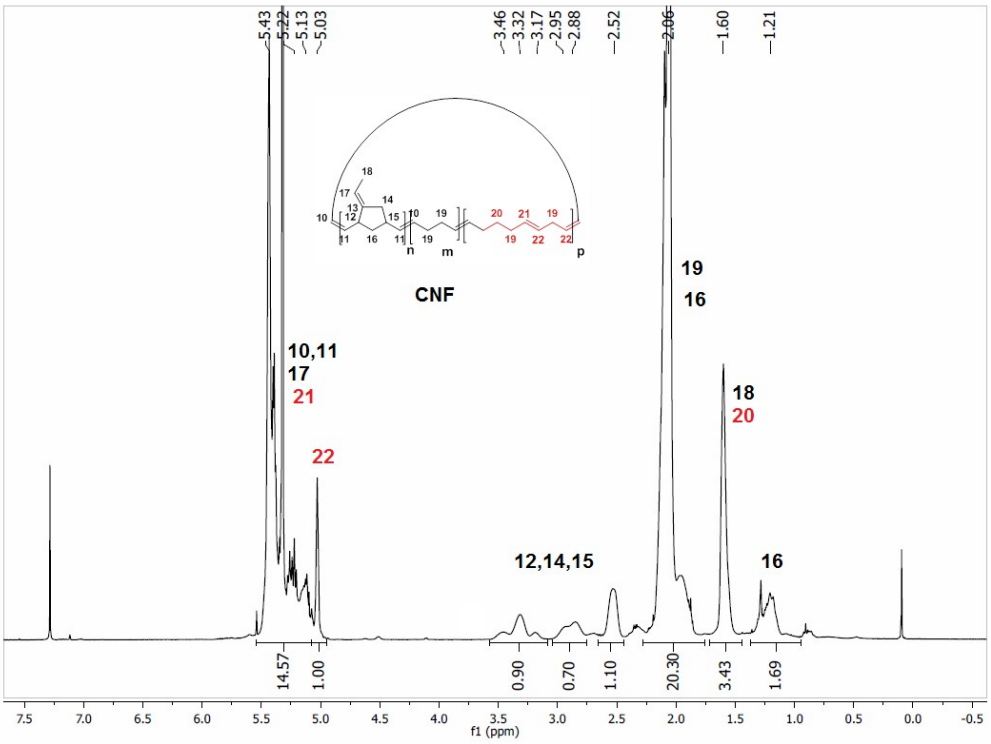

Fig. S16. ^{1}H NMR spectrum (400 MHz, $CDCl_3$, 23 °C) of **CNF** copolymer isolated from a crude copolymer prepared from ROMP/CM of ENB and CDT using **G2** and CTA **1** (Table 1, entry 4).

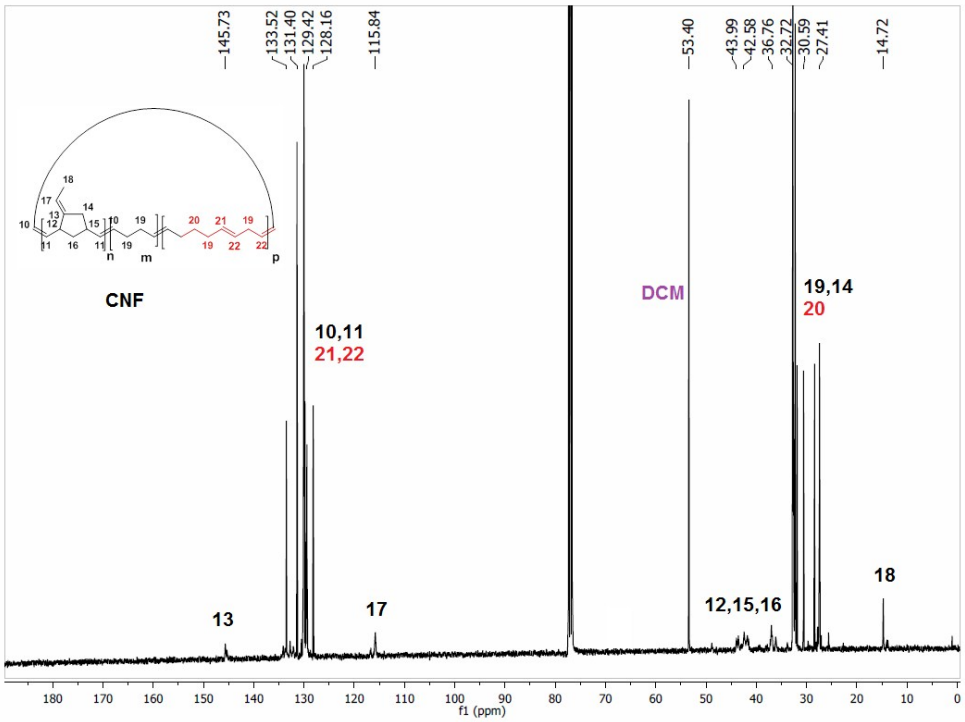

Fig. S17. $^{13}C\{^{1}H\}$ NMR spectrum (125 MHz, $CDCl_3$, 23 °C) of **CNF** copolymer isolated from a crude copolymer prepared from ROMP/CM of ENB and CDT using **G2** and CTA **1** (Table 1, entry 4).

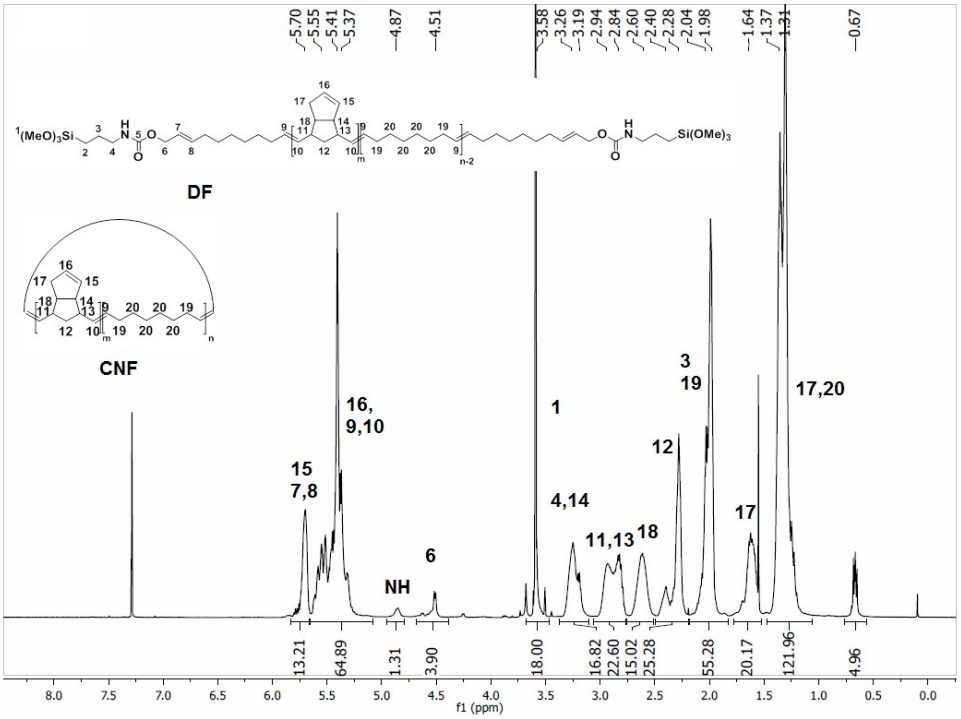

Fig.S18. ^{1}H NMR spectrum (500 MHz, $CDCl_3$, 23 °C) of a crude copolymer prepared from ROMP/CM of DCPD and COE using **G2** and CTA **1** (Table 1, entry 10).

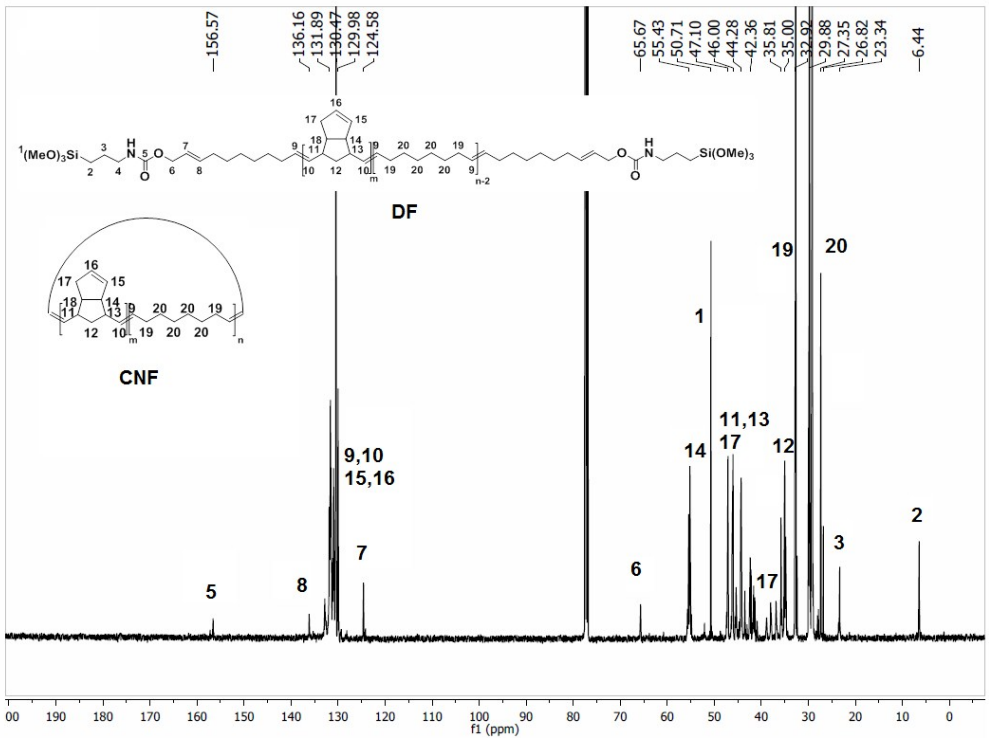

Fig.S19. $^{13}C\{^{1}H\}$ NMR spectrum (125 MHz, $CDCl_3$, 23 °C) of a crude copolymer prepared from ROMP/CM of DCPD and COE using **G2** and CTA **1** (Table 1, entry 10).

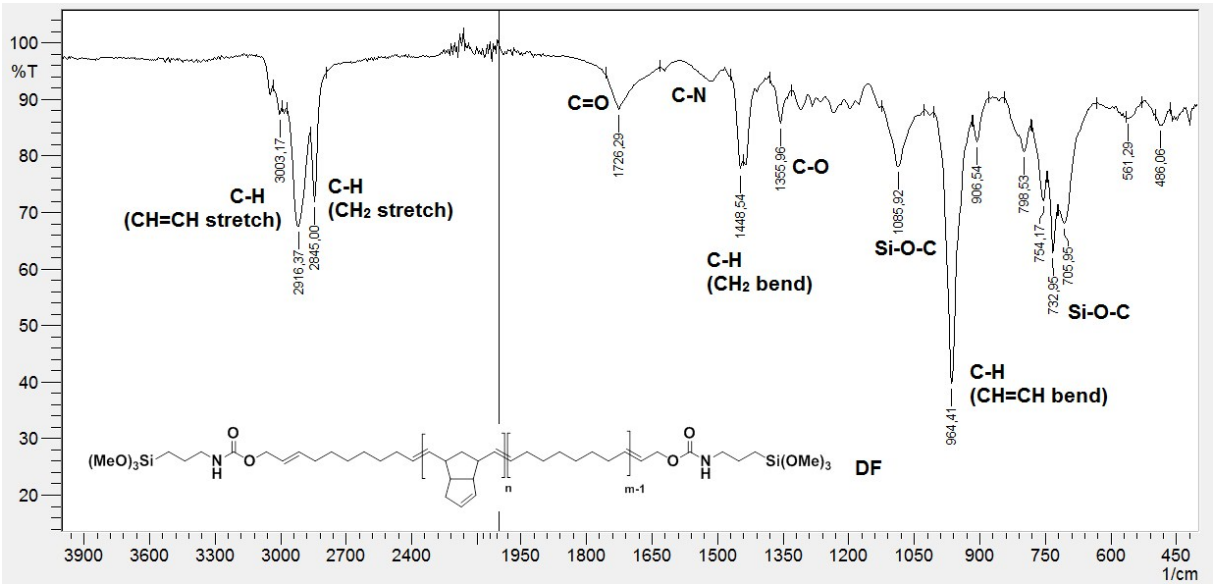

Fig. S20. FTIR spectrum of a crude copolymer prepared from ROMP/CM of DCPD and COE using **G2** and CTA **1** (Table 1, entry 10).

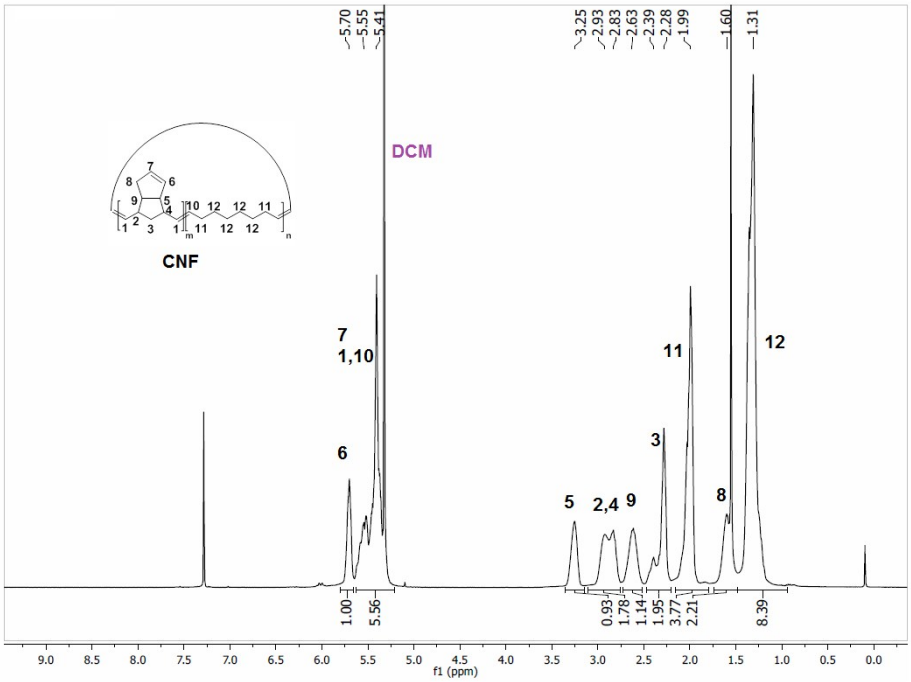

Fig. S21. ^{1}H NMR spectrum (500 MHz, $CDCl_3$, 23 °C) of **CNF** copolymer isolated from a crude copolymer prepared from ROMP/CM of DCPD and COE using **G2** and CTA **1** (Table 1, entry 10).

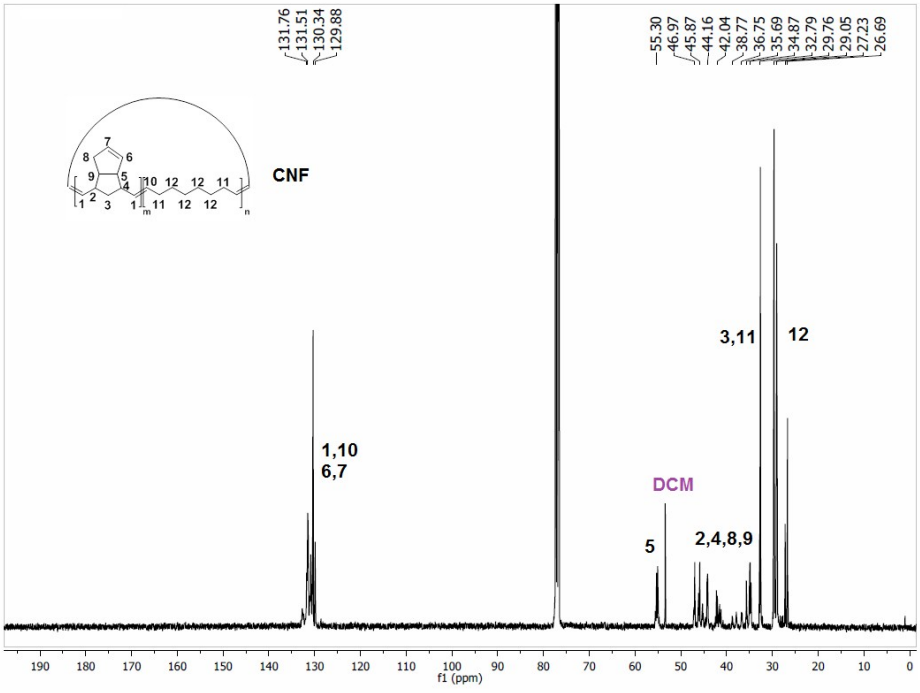

Fig.S22. $^{13}C\{^{1}H\}$ NMR spectrum (125 MHz, $CDCl_3$, 23 °C) of **CNF** copolymer isolated from a crude copolymer prepared from ROMP/CM of DCPD and COE using **G2** and CTA **1** (Table 1, entry 10).

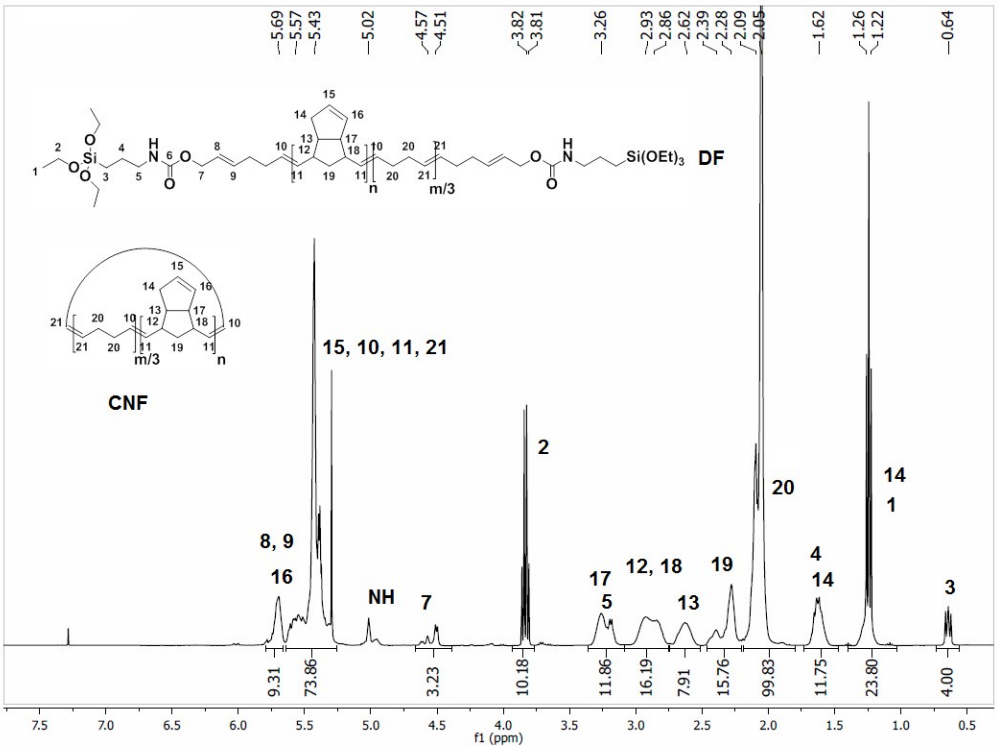

Fig. S23. ^{1}H NMR spectrum (500 MHz, $CDCl_3$, 23 °C) of a crude copolymer prepared from ROMP/CM of DCPD and CDT using **G2** and CTA **1** (Table 1, entry 12).

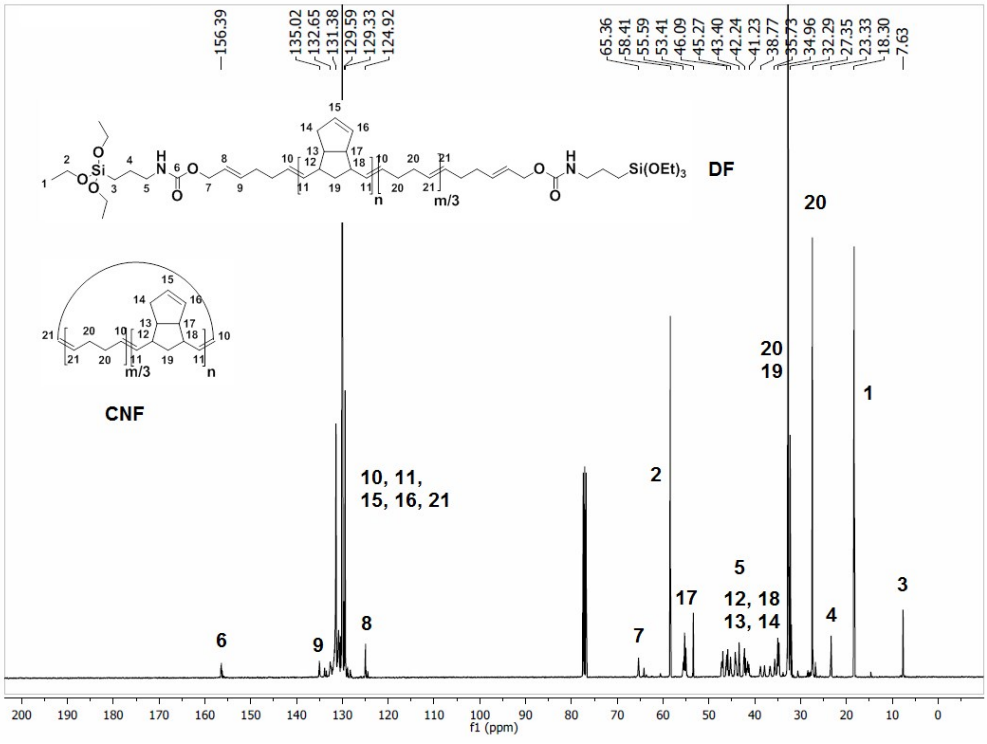

Fig. S24. ^{13}C{^{1}H} NMR spectrum (125 MHz, $CDCl_3$, 23 °C) of a crude copolymer prepared from ROMP/CM of DCPD and CDT using **G2** and CTA **1** (Table 1, entry 12).

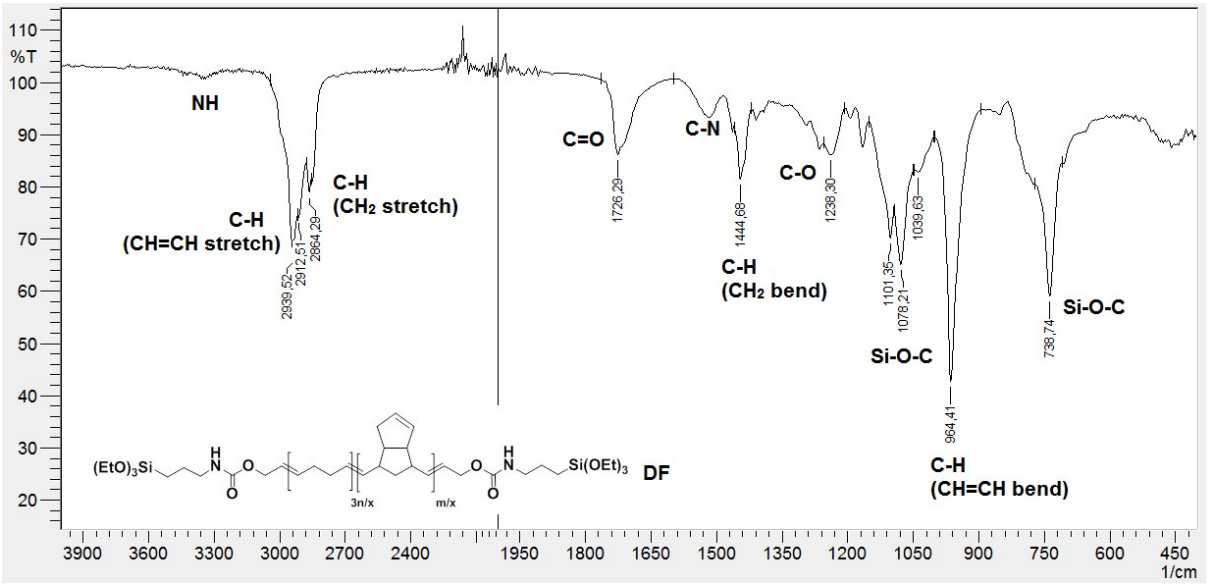

Fig. S25. FTIR spectrum of a crude copolymer prepared from ROMP/CM of DCPD and CDT using **G2** and CTA **1** (Table 1, entry 12).

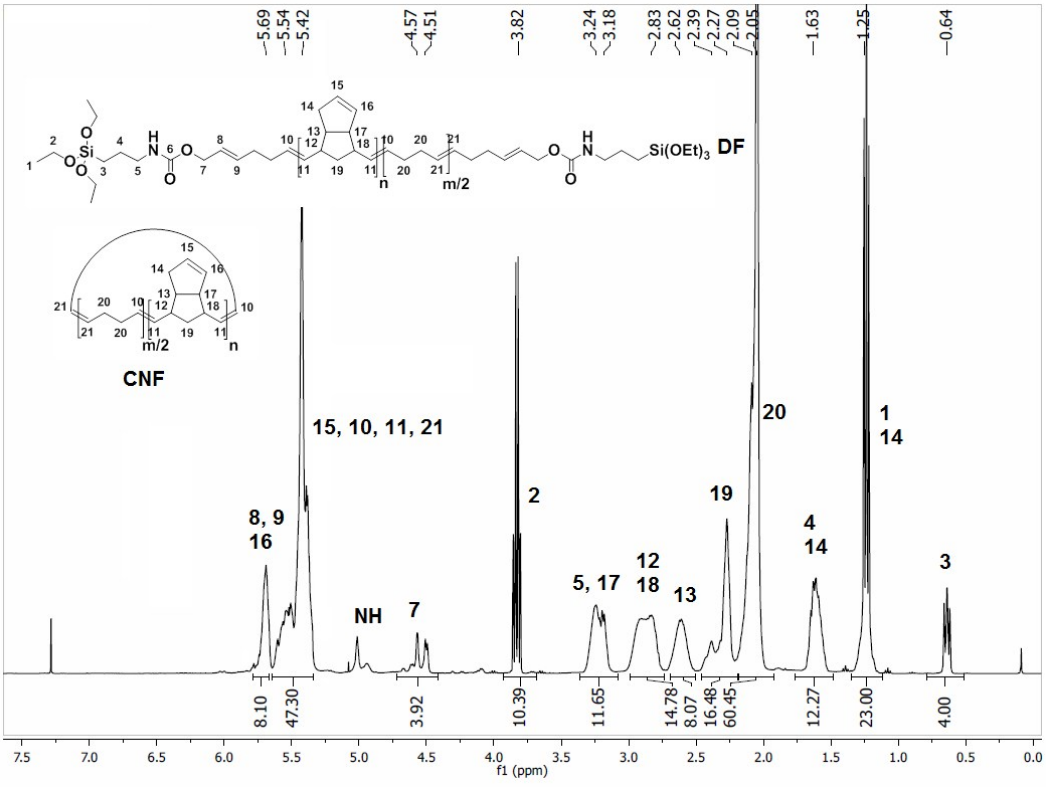

Fig. S26. ^{1}H NMR spectrum (500 MHz, $CDCl_3$, 23 °C) of a crude copolymer prepared from ROMP/CM of DCPD and COD using **G2** and CTA **1** (Table 1, entry 14).

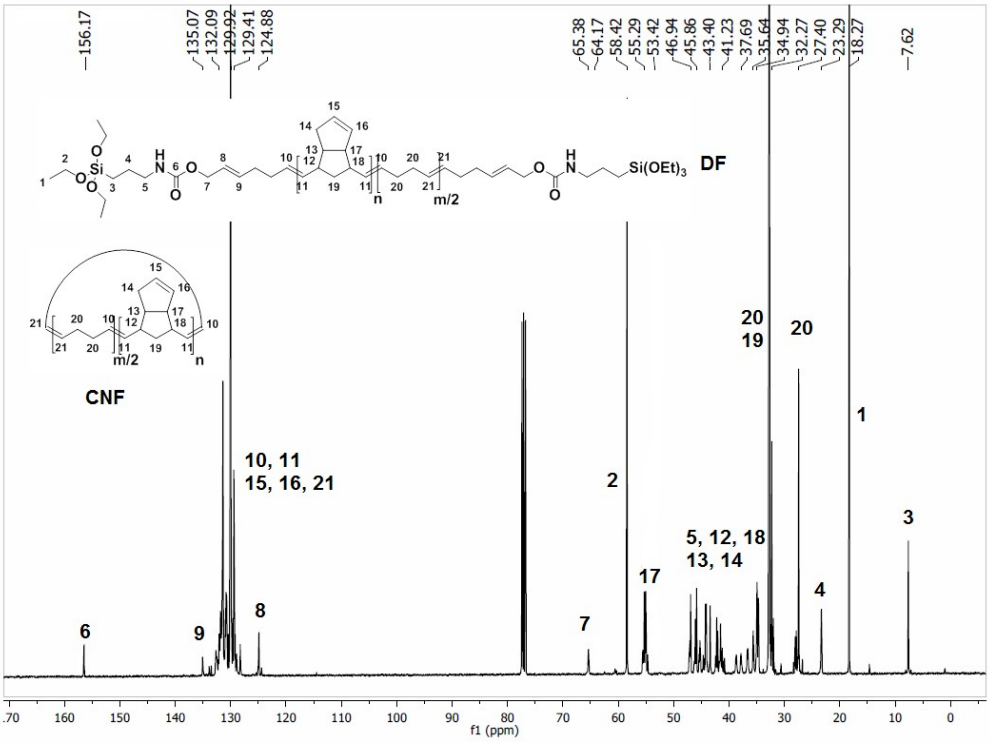

Fig. S27. $^{13}C\{^{1}H\}$ NMR spectrum (125 MHz, $CDCl_3$, 23 °C) of a crude copolymer prepared from ROMP/CM of DCPD and COD using **G2** and CTA **1** (Table 1, entry 14).

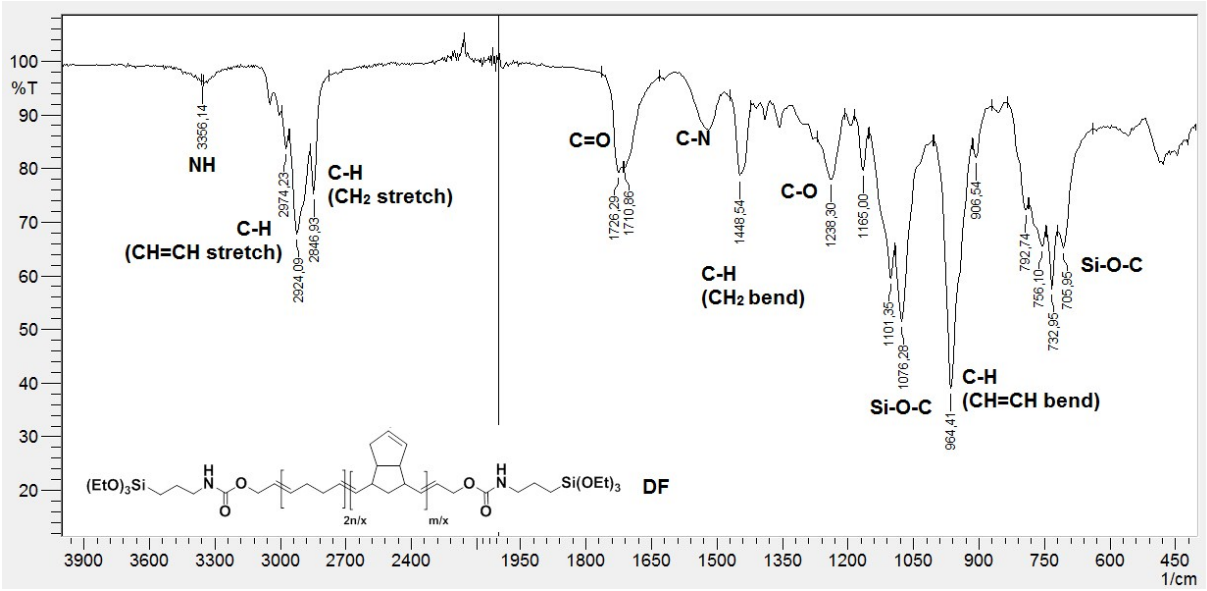

Fig. S28. FTIR spectrum of a crude copolymer prepared from ROMP/CM of DCPD and COD using **G2** and CTA **1** (Table 1, entry 14).

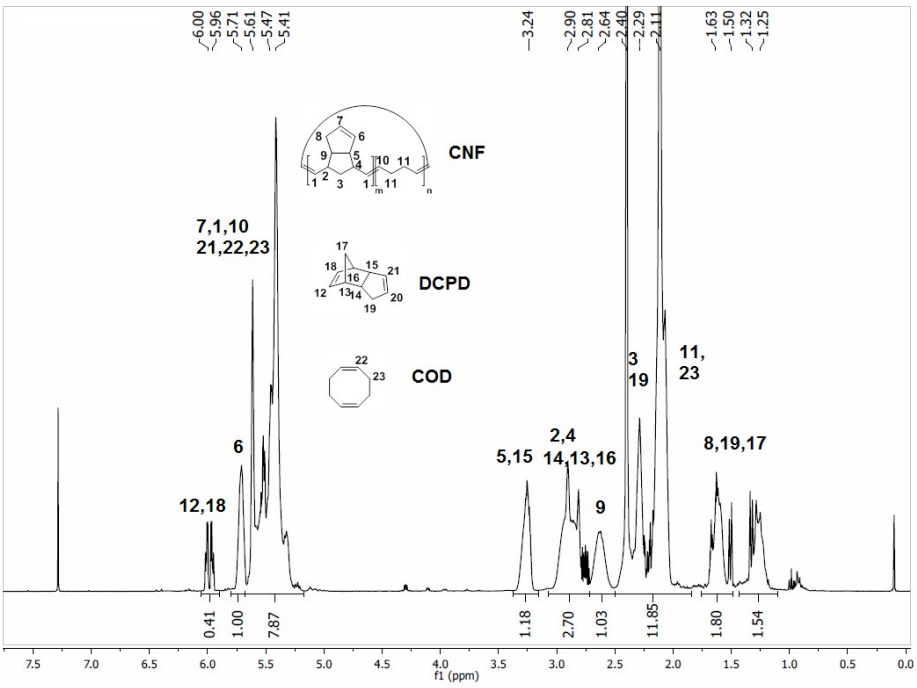

Fig. S29. ^{1}H NMR spectrum (500 MHz, $CDCl_3$, 23 °C) of **CNF** copolymer isolated from a crude copolymer prepared from ROMP/CM of DCPD and COD using **G2** and CTA **1** (Table 1, entry 14).

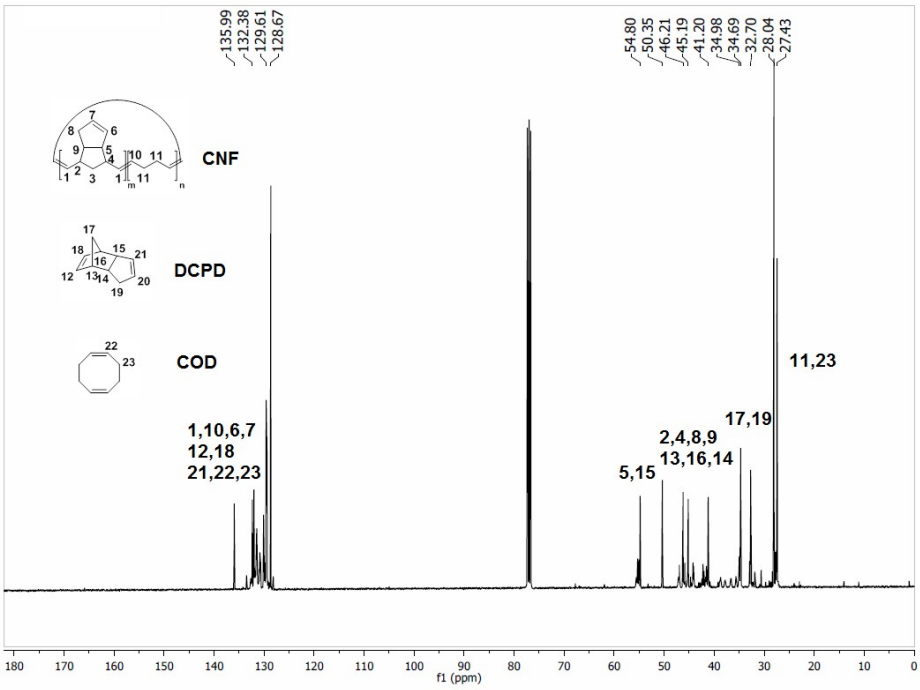

Fig. S30. ^{13}C{^{1}H} NMR spectrum (125 MHz, $CDCl_3$, 23 °C) of **CNF** copolymer isolated from a crude copolymer prepared from ROMP/CM of DCPD and COD using **G2** and CTA **1** (Table 1, entry 14).

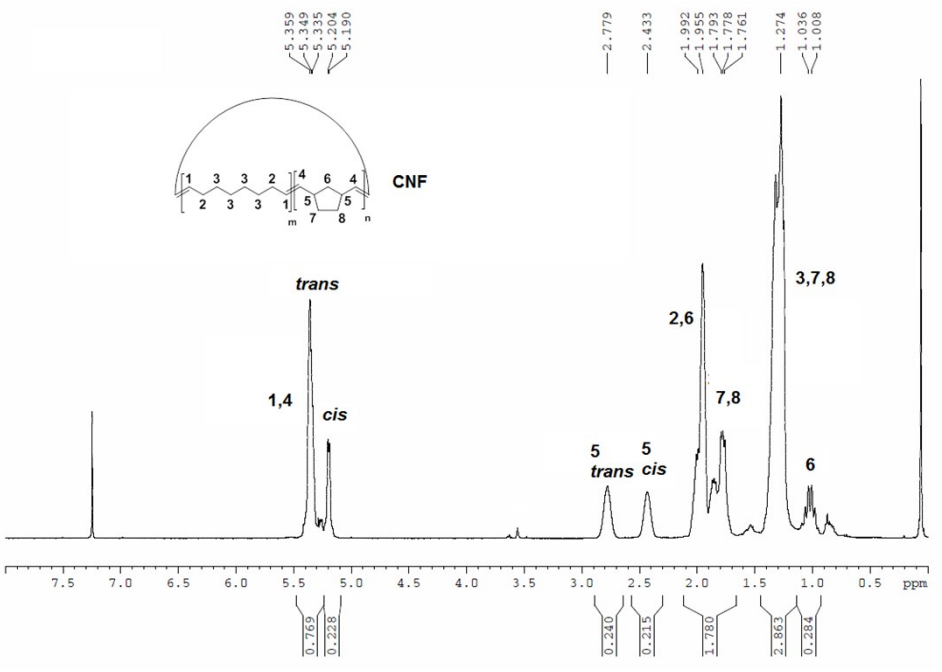

Fig. S31. ^{1}H NMR spectrum (400 MHz, $CDCl_3$, 23 °C) of **CNF** copolymer isolated from a crude copolymer prepared from ROMP/CM of NB and COE using **G2** and CTA **1-OEt** (Table 1, entry 1).

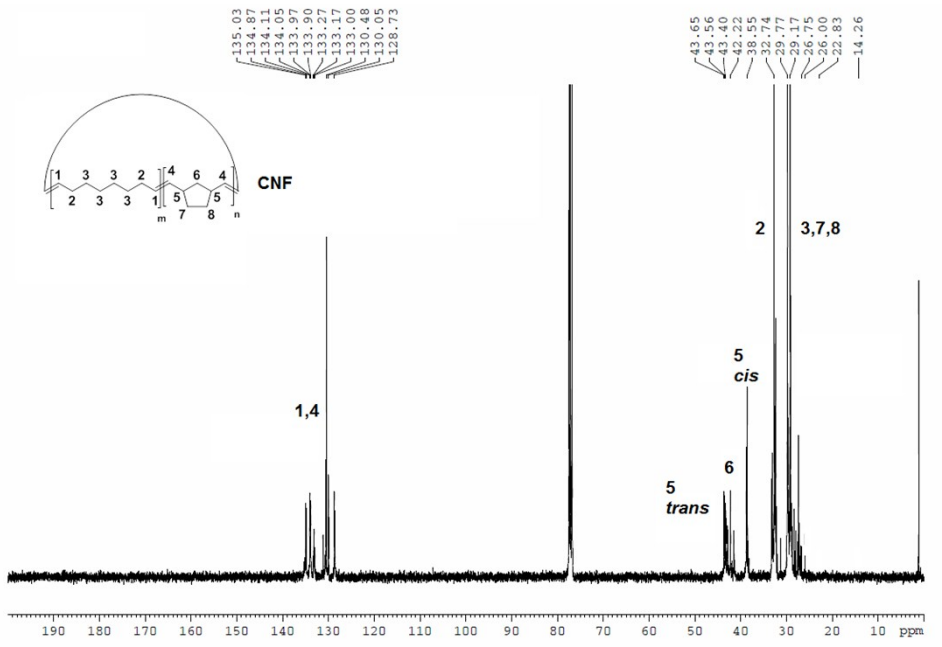

Fig. S32. ^{13}C NMR spectrum (100 MHz, $CDCl_3$, 23 °C) of **CNF** copolymer isolated from a crude copolymer prepared from ROMP/CM of NB and COE using **G2** and CTA **1-OEt** (Table 1, entry 1).

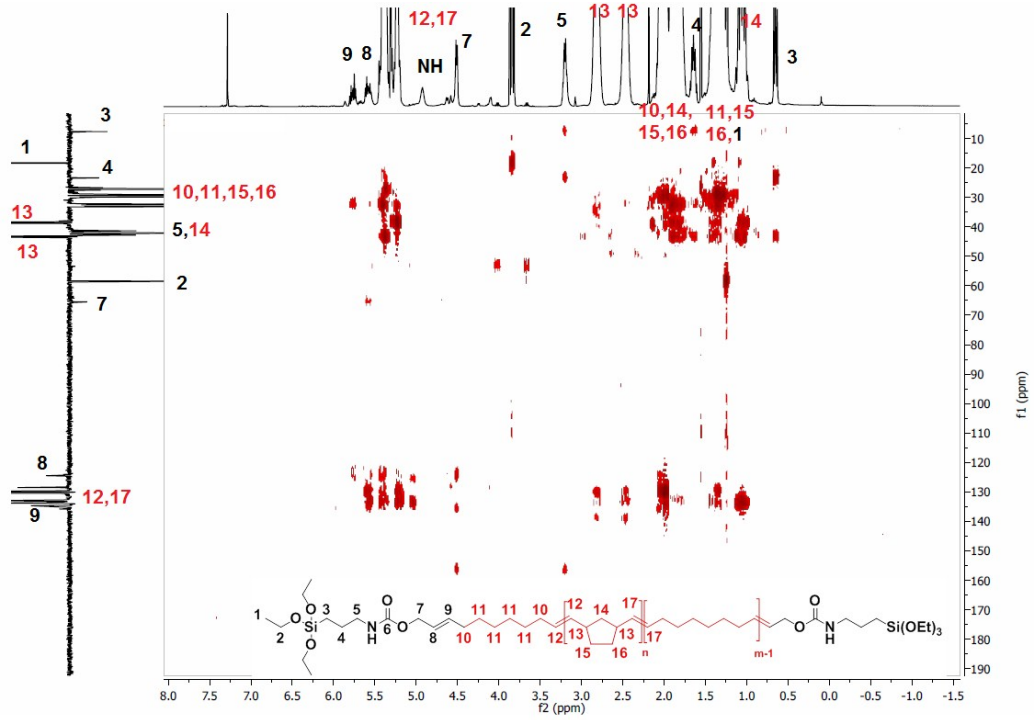

Fig. S33. ^{1}H-$^{13}C\{^{1}H\}$ HMBC (DEPT) NMR spectrum (400 MHz, $CDCl_3$, 23 °C) of a crude copolymer prepared from ROMP/CM of NB and COE using **G2** and CTA **1** (Table 1, entry 1).

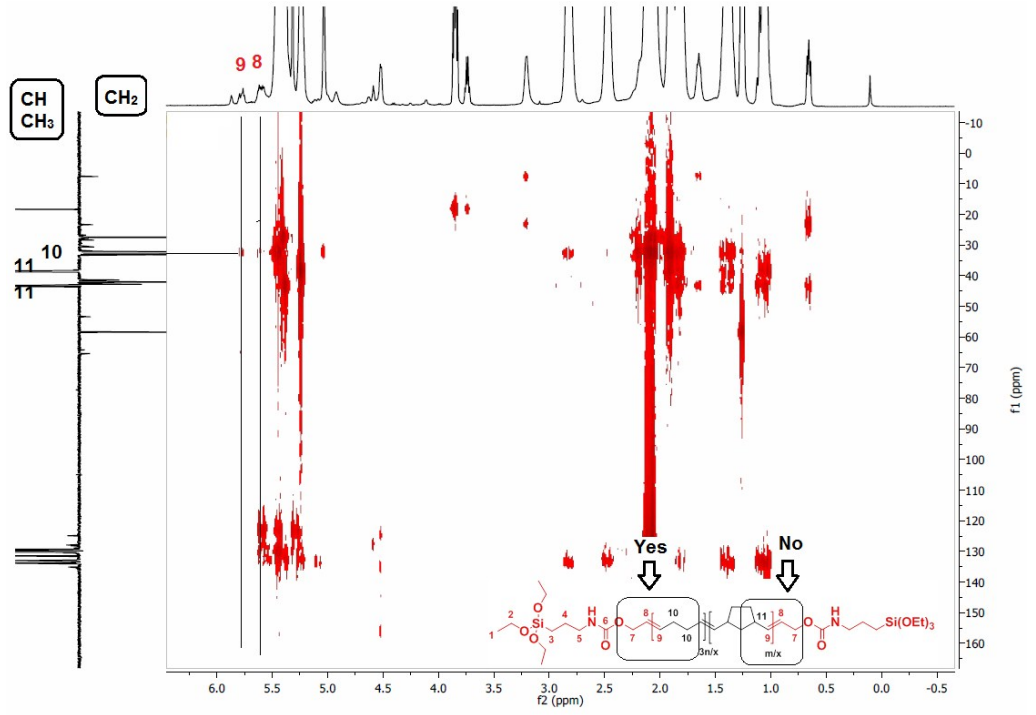

Fig. S34. ^{1}H-^{13}C HMBC (DEPT) NMR spectrum (400 MHz, $CDCl_3$, 23 °C) of a crude copolymer prepared from ROMP/CM of NB and CDT using **G2** and CTA **1** (Table 1, entry 3; spectrum with assignments of all signals in Fig. S35).

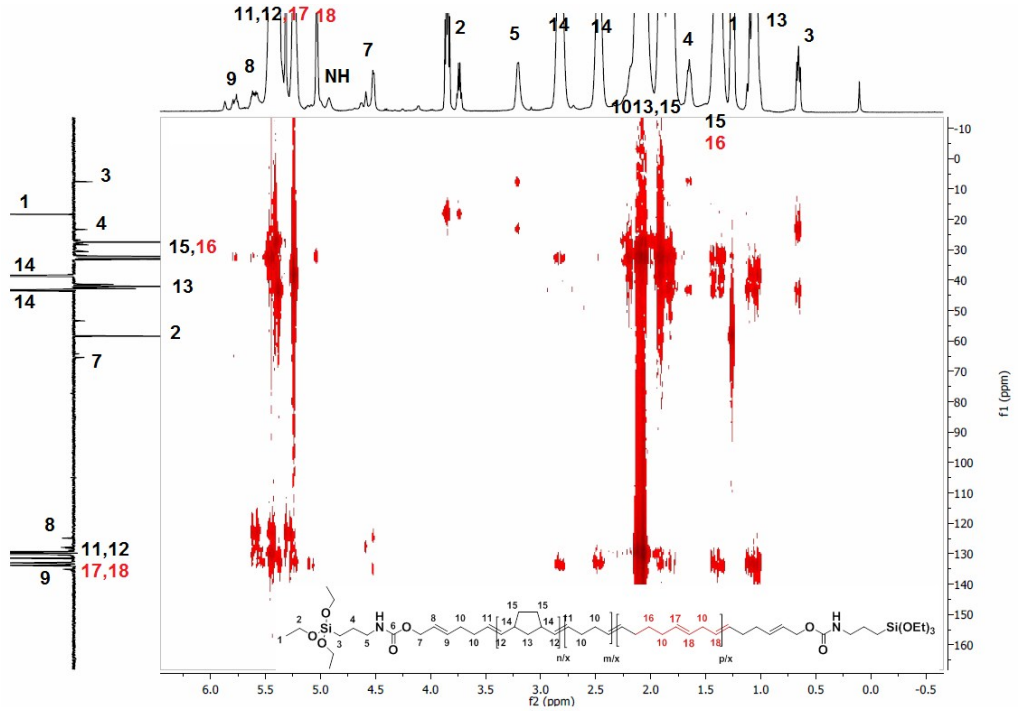

Fig. S35. ^{1}H-^{13}C HMBC (DEPT) NMR spectrum (400 MHz, $CDCl_3$, 23 °C) of a crude copolymer prepared from ROMP/CM of NB and CDT using **G2** and CTA **1** (Table 1, entry 3).

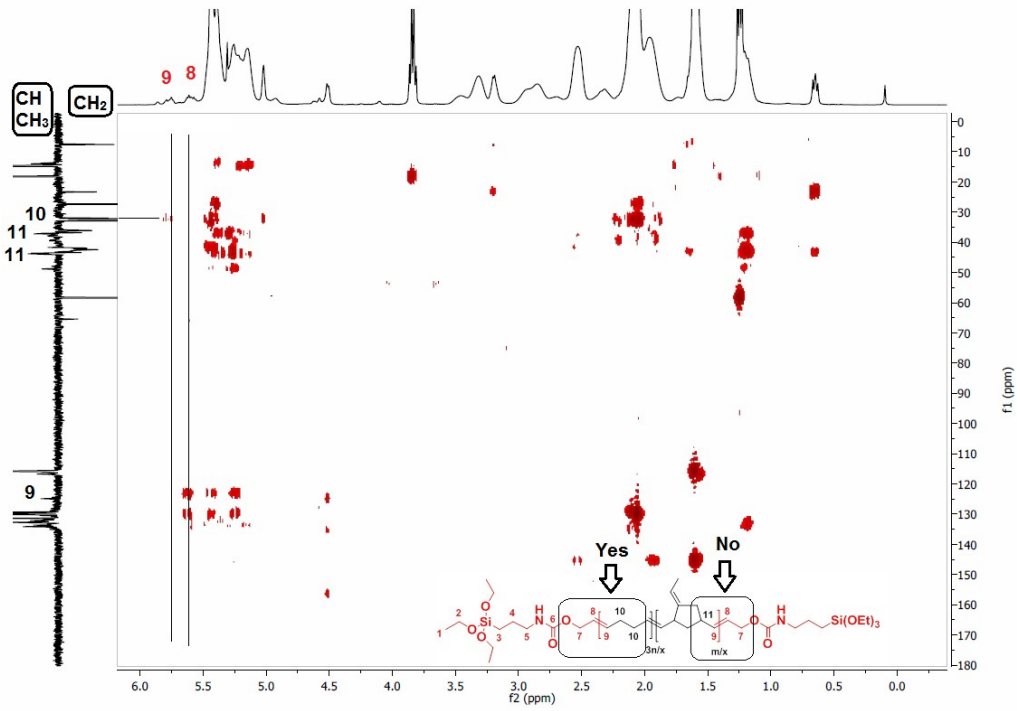

Fig. S36. ^{1}H-^{13}C HMBC (DEPT) NMR spectrum (400 MHz, $CDCl_3$, 23 °C) of a crude copolymer prepared from ROMP/CM of ENB and CDT using **G2** and CTA **1** (Table 1, entry 4; spectrum with assignments of all signals in Fig. S37).

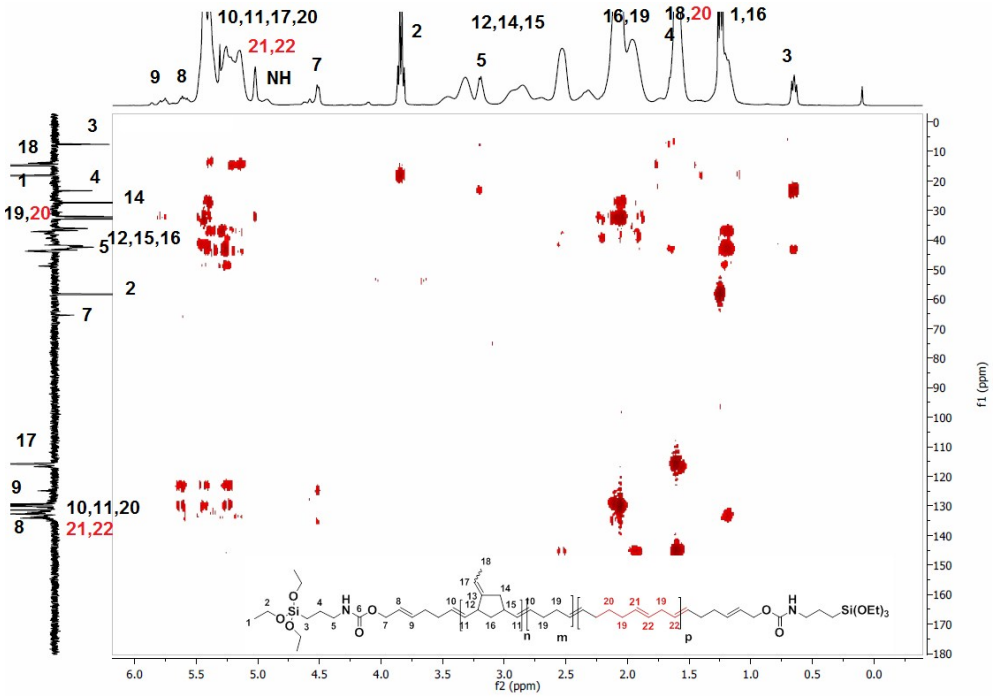

Fig. S37. ^{1}H-^{13}C HMBC (DEPT) NMR spectrum (400 MHz, $CDCl_3$, 23 °C) of a crude copolymer prepared from ROMP/CM of ENB and CDT using **G2** and CTA **1** (Table 1, entry 4).

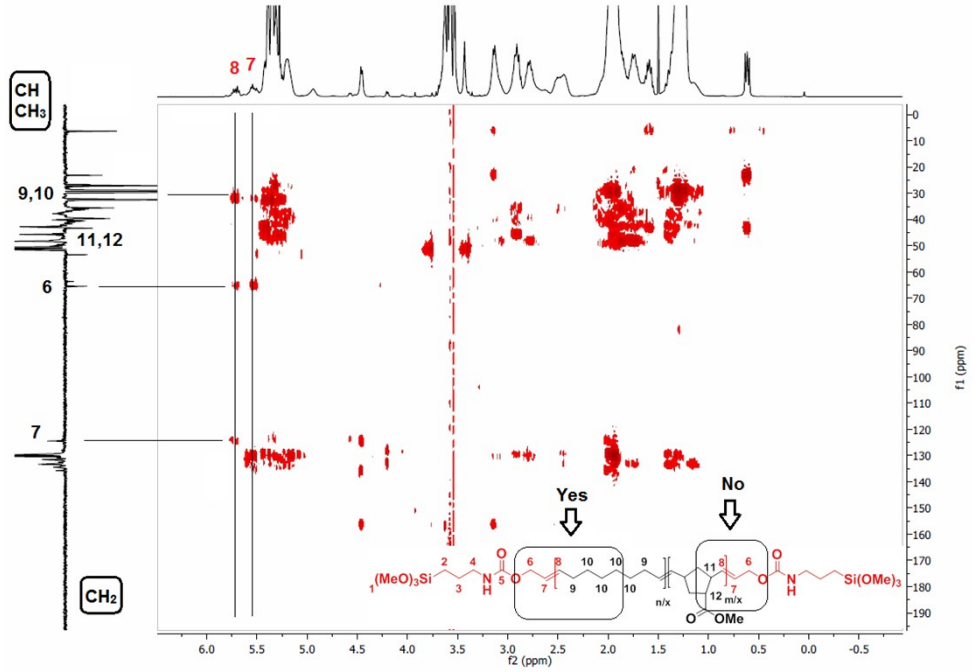

Fig. S38. ^{1}H-^{13}C HMBC (DEPT) NMR spectrum (400 MHz, $CDCl_3$, 23 °C) of a crude copolymer prepared from ROMP/CM of oxaNB^{COOMe} and COE using **G2** and CTA **1** (Table 1, entry 8; spectrum with assignments of all signals in Fig.S39).

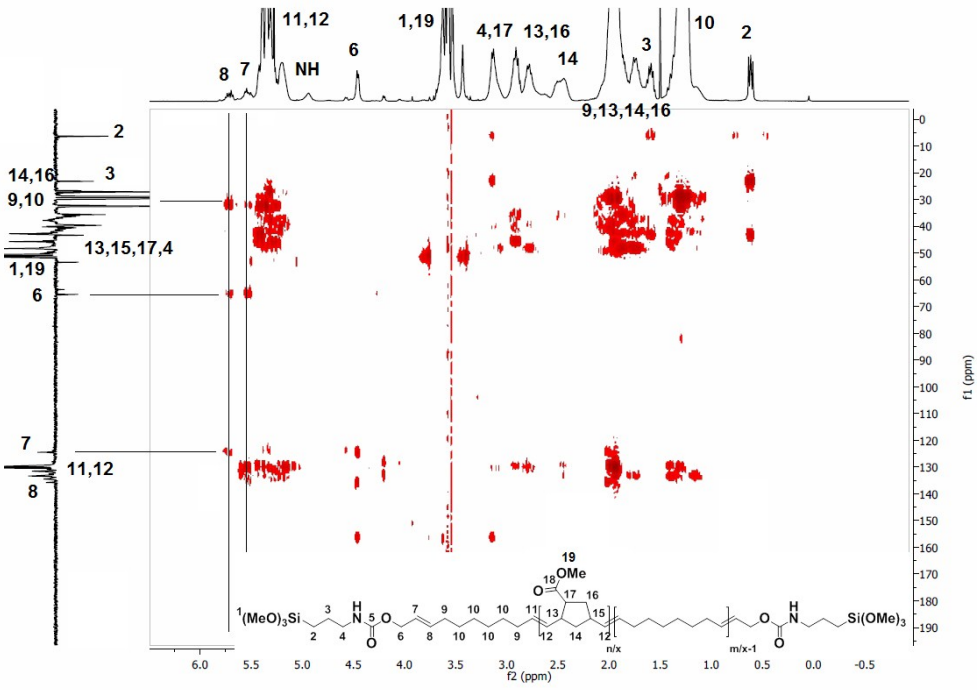

Fig. S39. ^{1}H-^{13}C HMBC (DEPT) NMR spectrum (400 MHz, $CDCl_3$, 23 °C) of a crude copolymer prepared from ROMP/CM of oxaNB^{COOMe} and COE using **G2** and CTA **1** (Table 1, entry 8).

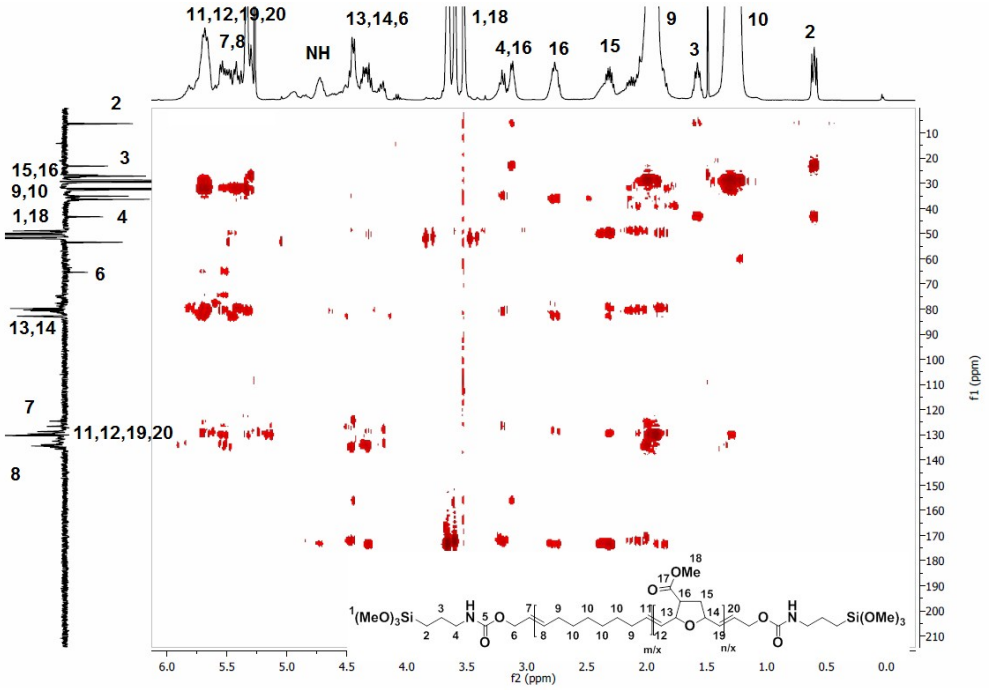

Fig. S40. ^{1}H-^{13}C (DEPT) HMBC NMR spectrum (400 MHz, $CDCl_3$, 23 °C) of a crude copolymer prepared from ROMP/CM of oxaNB^{COOMe}/COE using **G2** and CTA **1** (Table 1, entry 10).

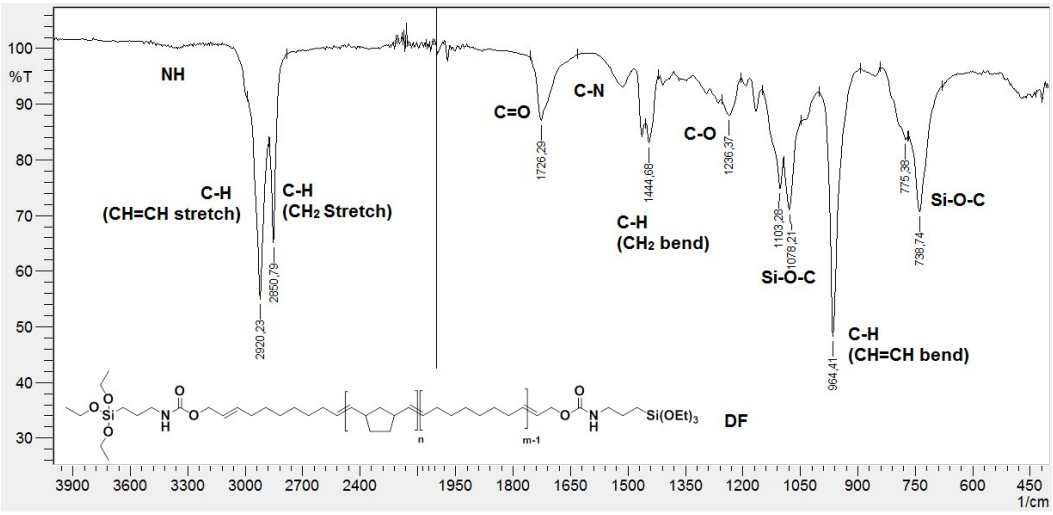

Fig. S41. FTIR spectrum of a crude copolymer prepared from ROMP/CM of NB and COE using **G2** and CTA **1** (Table 1, entry 1).

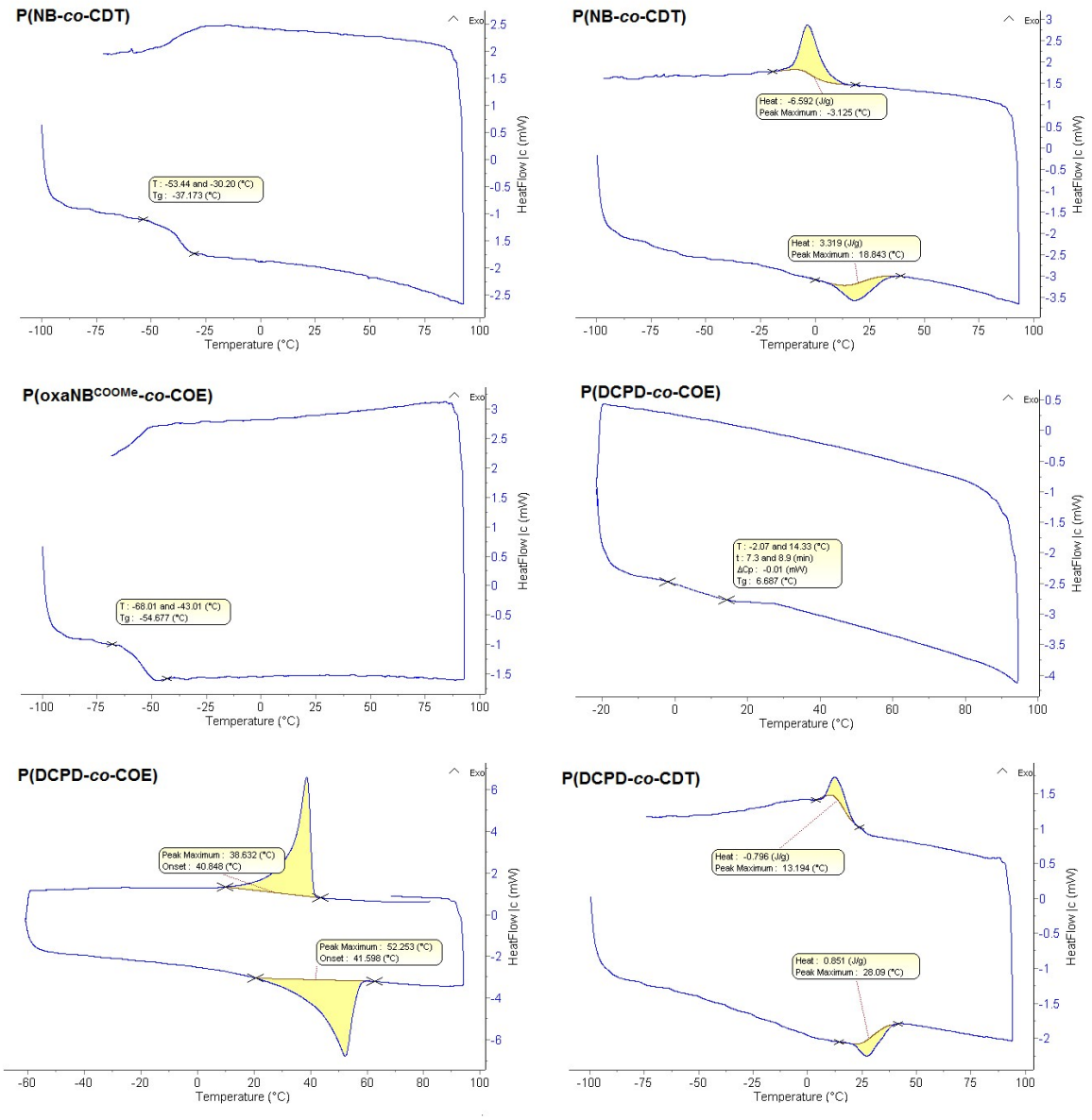

Fig. S42. DSC traces of copolyolefin samples prepared from the ROMP/CM of NB/CDT, oxaNB^{COOMe}/COE, DCPD/COE and DCPD/CDT using **G2** catalyst and CTA **1** (Table 2, entries 4, 6, 19, 24, 26, 31).

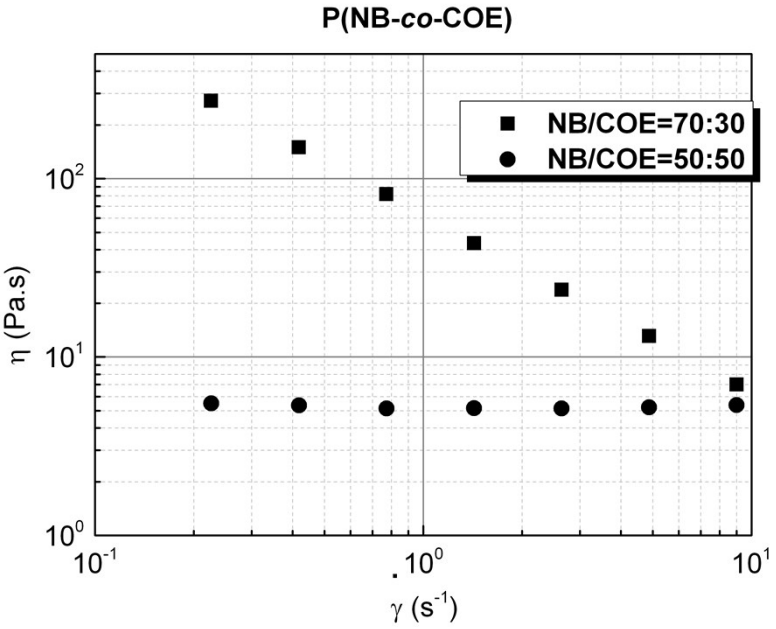

Fig. S43. Flow curves of copolyolefin samples prepared from the ROMP/CM of NB/COE, using **G2** catalyst and CTA **1** (Table 3, entries 1 and 2).

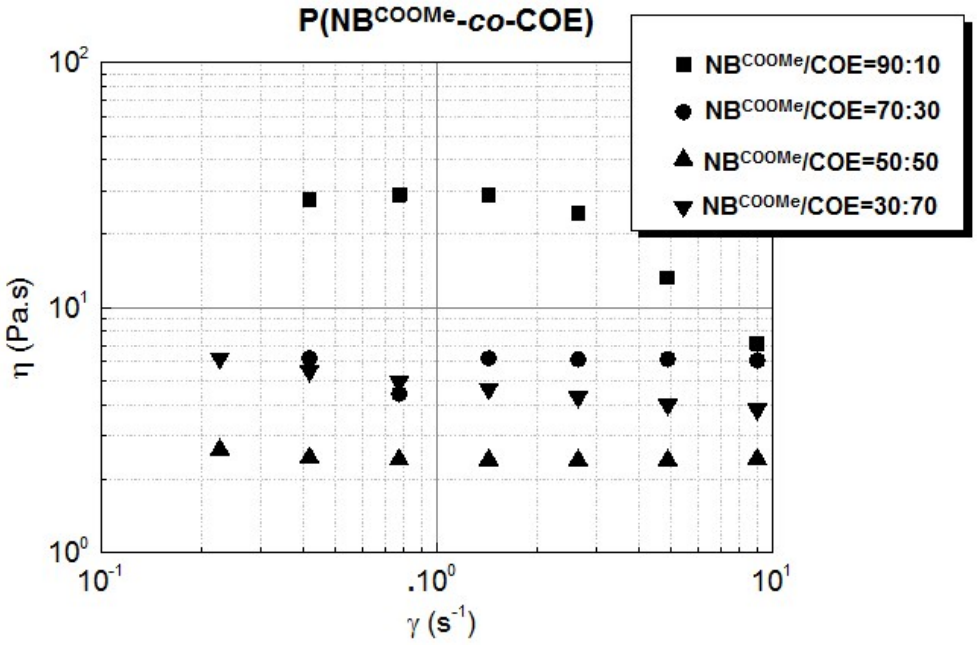

Fig. S44. Flow curves of copolyolefin samples prepared from the ROMP/CM of NB^{COOMe}/COE using **G2** catalyst and CTA **1** (Table 3, entries 3–6).

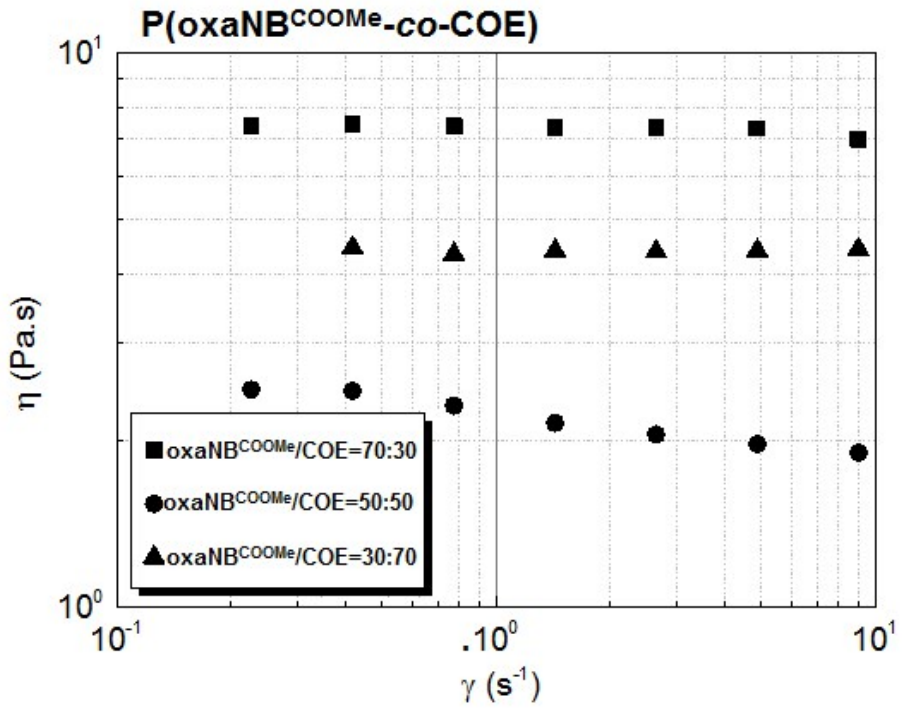

Fig. S45. Flow curves of copolyolefin samples prepared from the ROMP/CM of oxaNB^{COOMe}/COE using **G2** catalyst and CTA **1** (Table 3, entries 7–9).

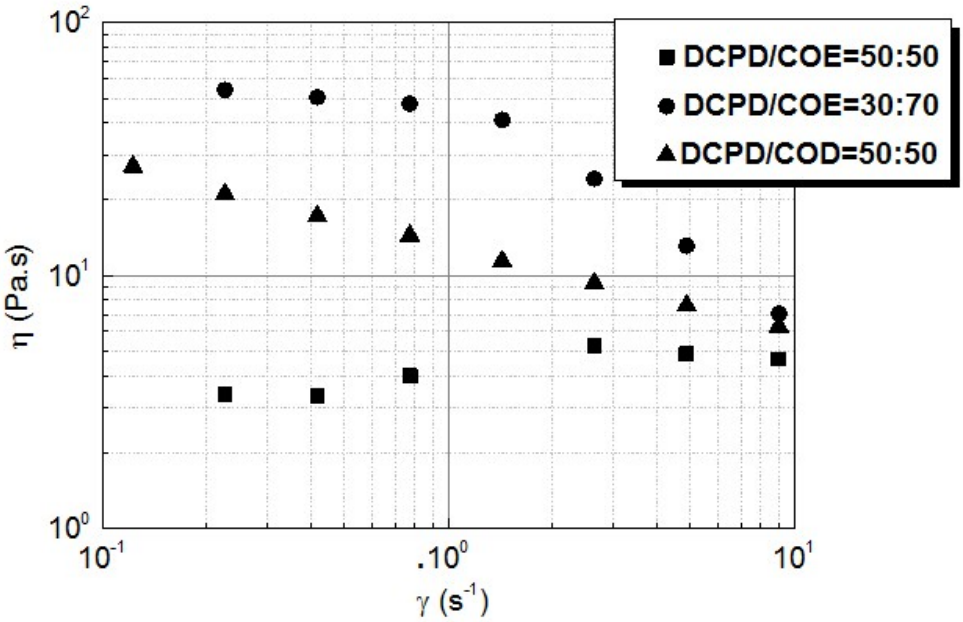

Fig. S46. Flow curves of copolyolefin samples prepared from the ROMP/CM of DCPD/COE and DCPD/COD using **G2** catalyst and CTA **1** (Table 3, entries 10–12).

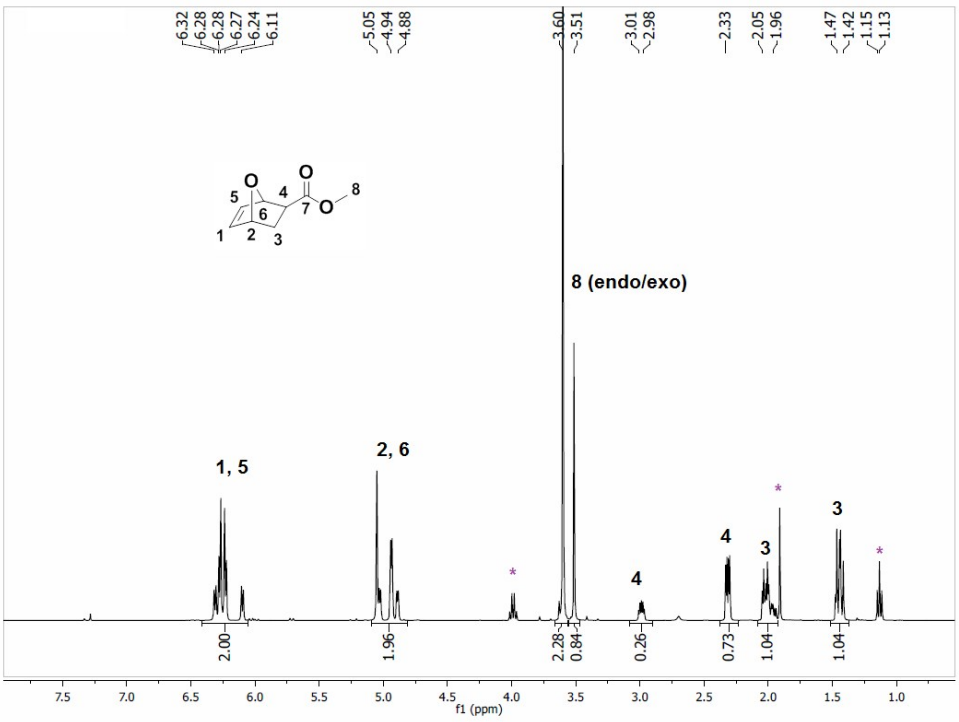

Fig. S47. ^{1}H NMR spectrum (500 MHz, $CDCl_3$, 23 °C) of oxaNB^{COOMe}.

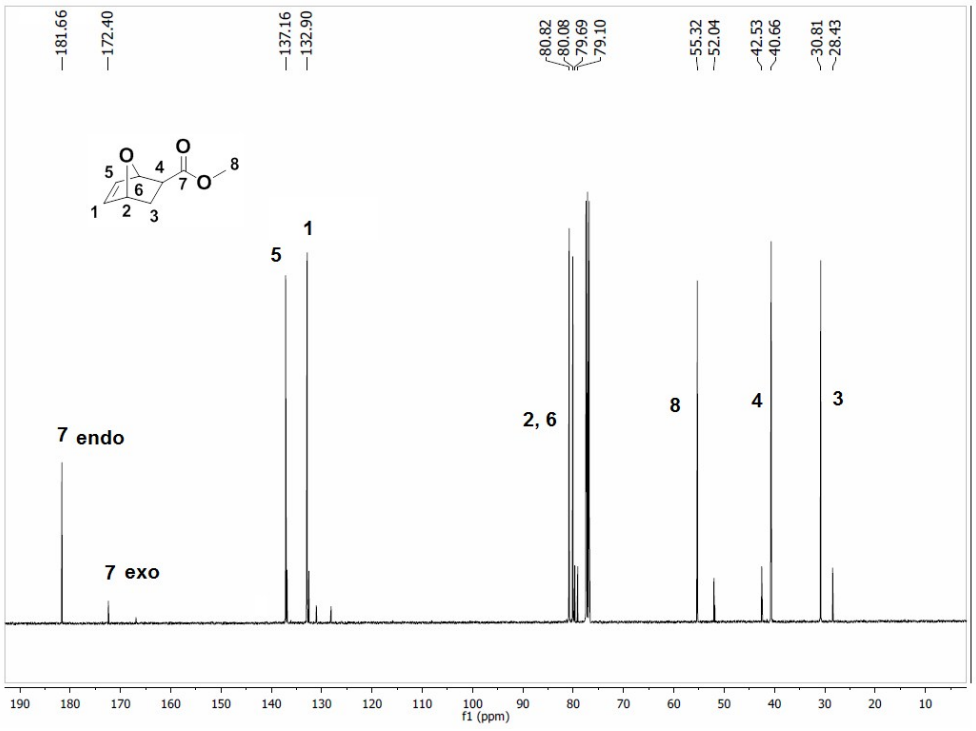

Fig. S48. $^{13}C\{^{1}H\}$ NMR spectrum (125 MHz, $CDCl_3$, 23 °C) of oxaNB^{COOMe}.